“The Development and Implementation of Low-Level Control Strategies for a Robust and Effective Low-Cost Rehabilitation Robot for Home Use”

PhD Transfer Report

Adam Metcalf

Supervisors:
Prof Martin Levesley
Dr Andrew Jackson
Dr Justin Gallagher

May 2019

Abstract

This report summarises the work done in the first 9 months of the PhD process as part of the requirement to transfer from Provisional PhD student to PhD student. The motivation for the project is to develop and implement low-level control schemes for a robust and low-cost rehabilitation robot for home installation after Stroke.

The literature review explored the current state of post-Stroke upper limb rehabilitation robotics and showed that there is a requirement for low-cost rehabilitation robotics, since the cost/benefit ratio of current commercial rehabilitation robotic solutions cannot be justified.

The report shows progress completed in the development of a low-cost integrated force sensor and end effector for the MyPAM robot, the justification of the selection of a Minimum Jerk Trajectory and the design of an Admittance Control scheme. Further work is discussed, including improvements to the force sensor and necessary work to implement both an Admittance control scheme and an Impedance control scheme.

Nomenclature

AR	Altered Reality
CTE	Cognitive Therapeutic Exercise
DoF	Degrees of Freedom
EEULRebot	End Effector Upper Limb Rehabilitation Robot
FEA	Finite Element Analysis
FPGA	Field Programmable Gate Array
hCAAR	home-based Computer Aided Arm Rehabilitation
iPAM	intelligent Pneumatic Arm Movement
MEMOS	Mechatronic System for Motor Recovery After Stroke
MIME	Mirror Image Motion Enabler
OS	Operating System
PC	Personal Computer
PNF	Proprioceptive Neuromuscular Facilitation
RATULS	Robot Assisted Training for the Upper Limb after Stroke
RTOS	Real Time Operating System
RUPERT	Robotic assisted Upper Extremity Repetitive Therapy
SCARA	Selective Compliance Assembly Robot Arm
sEMG	Surface Electromyography
VR	Virtual Reality

List of figures

List of Tables

Contents

Chapter 1: Introduction

1.1. Motivation

The likelihood of having a Stroke increases with age. Statistics show that the population of the UK is aging, due in part to an increase in life expectancy. This means that Stroke is becoming more prevalent in the UK, and this is a trend reflected across much of the Western world. In the UK the increase in Stroke prevalence places a large burden on the NHS and rehabilitation services, especially considering that it is understood that effective neural rehabilitation should be intensive and occur early after the onset of Stroke. In order to ease the burden on medical services and provide more access to therapy, research is increasingly focused on the use of robotics.

Rehabilitation robotics for the rehabilitation of neurological traumas such as Stroke are designed to assist the patient with training exercises, and by necessity focus on specific target areas. Gait trainers assist with walking rehabilitation, for example, and upper limb devices assist with reaching exercise training. The benefits of rehabilitation robotics are that repeatable, measurable and consistent training exercises can be provided alongside traditional human-led physiotherapy. This comes at the cost of systems which are expensive and therefore only appropriate to install in community settings such as hospitals, which limits the access to important rehabilitation. Whilst there has been some research into low cost robotic systems, commercially available rehabilitation robots cost in excess of $100,000.

1.2. Current MyPAM Rehabilitation Robot

The MyPAM (formerly hCAAR) is a 2 Degree of Freedom (DoF) planar robot for upper limb rehabilitation after neurological trauma. The robot is a powered arm which assists the user to reach targets. Visual feedback is provided by a screen. The MyPAM is shown by figure 1.1:

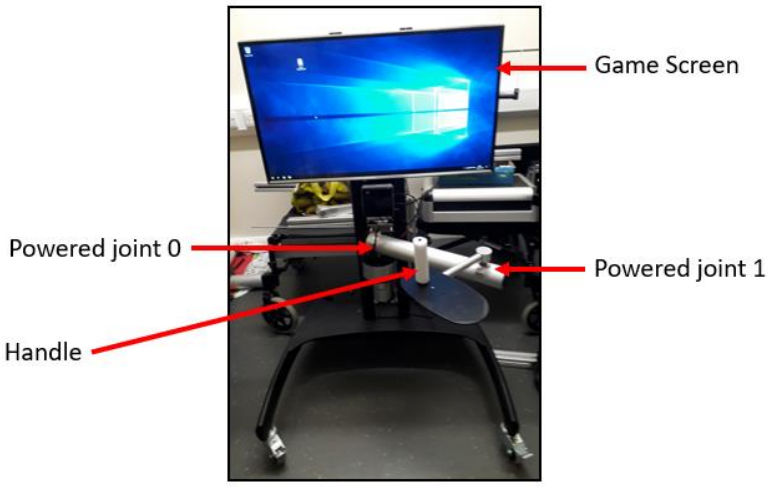

Figure 1.1: *The MyPAM rehabilitation robot.*

The MyPAM was first designed to assist in the rehabilitation of children with Cerebral Palsy, but in recent years the research focus has shifted to rehabilitation after Stroke. The MyPAM is designed to be a low-cost device in order to ensure that it is economic to install in the homes of patients. The MyPAM has been proven to be robust and effective but is currently suitable for use by patients with medium to high levels of motor control. It is expected that the implementation of more advanced low-level control schemes will extend the rehabilitation potential to patients with a greater level of disability.

1.2.1. Architecture

The MyPAM currently consists of a game environment, written using Unity® software. The game acts as a high-level controller and generates reaching tasks which aim to fulfil rehabilitation goals. Low-level control is achieved using a National Instruments myRIO, which generates the motor demands and performs the data acquisition required for feedback control via a Field Programmable Gate Array (FPGA) chip. Each of the 2 joints is powered by a Maxon brushed DC motor and position feedback for each joint is provided by an ENX encoder integrated into the motor. Much of the cost of the MyPAM currently resides in the use of National Instruments hardware and software. A block diagram showing the current system architecture is shown by figure 1.2:

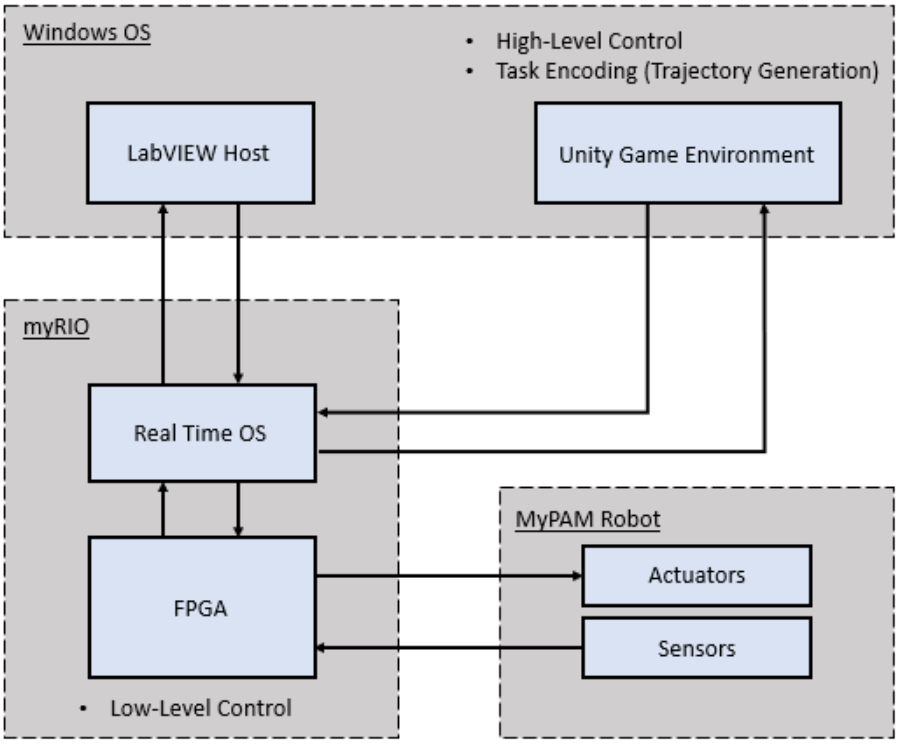

Figure 1.2: *A block diagram showing the system architecture of the current MyPAM.*

1.2.2. Trajectory Generation and Low-Level Control

In the current MyPAM system the game is responsible for generating the trajectory for each reaching movement, running at 30Hz on the host PC. The game creates the final

target position according to a high-level control strategy and generates equidistant intermediate positions between the start position and the final position as a linear path, as shown by figure 1.3:

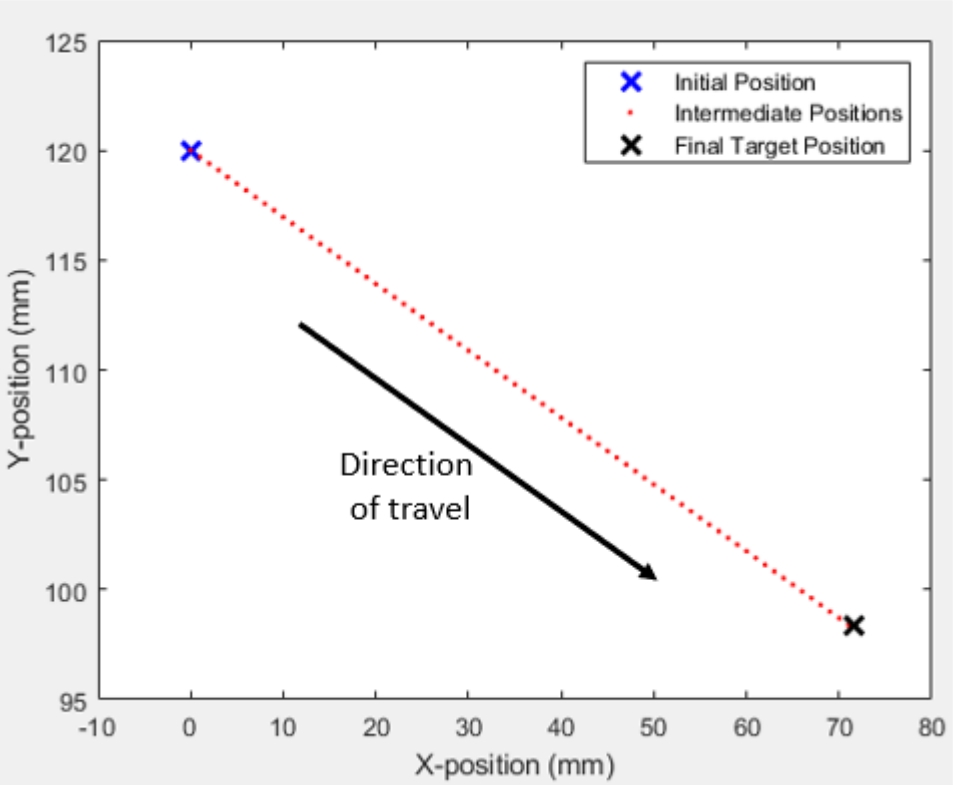

Figure 1.3: *An example of a linear trajectory generated by the game.*

These intermediate positions are passed one at a time to the myRIO running LabVIEW, which acts as the low-level controller. The myRIO, operating at 500Hz on a Real Time Operating System (RTOS), is only aware of the current position and the next intermediate position. Using position PID control, the myRIO generates the motor demands. This can be considered as a highly coupled arrangement, since there is a dependence on reliable and timely communication between the game and the low-level controller to ensure correct and safe operation of the MyPAM. Position PID is used, rather than a control scheme which modulates interaction forces between the robot and the patient as a cost saving effort, since reliable industrial force sensors are expensive.

1.3. Aims and Objectives

Aim:

- To develop and implement Admittance Control and Impedance Control strategies for a robust and low-cost rehabilitation robot suitable for home use.

Objectives:

- Develop, test, and validate a low-cost force sensor for the end effector.
- Integrate the low-cost force sensor into the systems architecture of the MyPAM.

- Develop, test, and validate a smooth trajectory generator with attractors and repulsors.
- Integrate the trajectory generator into the software architecture of the MyPAM.
- Develop, test, and validate a low-cost torque sensor for the MyPAM powered joints.
- Integrate the low-cost torque sensors into the systems architecture of the MyPAM.
- Design, implement, test, and validate an Admittance Control scheme.
- Design, implement, test, and validate an Impedance Control scheme.
- Determine the effectiveness of the Admittance Control scheme in human based trials.
- Determine the effectiveness of the Impedance Control scheme in human based trials.

Chapter 2: Literature Review

2.1. Stroke

2.1.1. Stroke Mechanisms and Effects

Stroke, also known as Cerebrovascular Accident, is the leading cause of disability in the UK according to the Stroke Association (2018). Stroke is classified by 2 mechanisms: Haemorrhagic Stroke and Ischaemic Stroke. Haemorrhagic Stroke occurs when an artery in the brain ruptures, often as a result of high blood pressure. Ischaemic Stroke occurs due to the blockage of an artery in the brain, usually caused by a blood clot or fatty deposits. Both mechanisms lead to cell damage or cell death in the affected region of the brain because of a lack of oxygen (Moskowitz et al, 2010).

The symptoms of Stroke are wide ranging and dependant on which region of the brain has been affected and the severity of the Stroke. Different regions of the brain control different behaviour, as shown by figure 2.1:

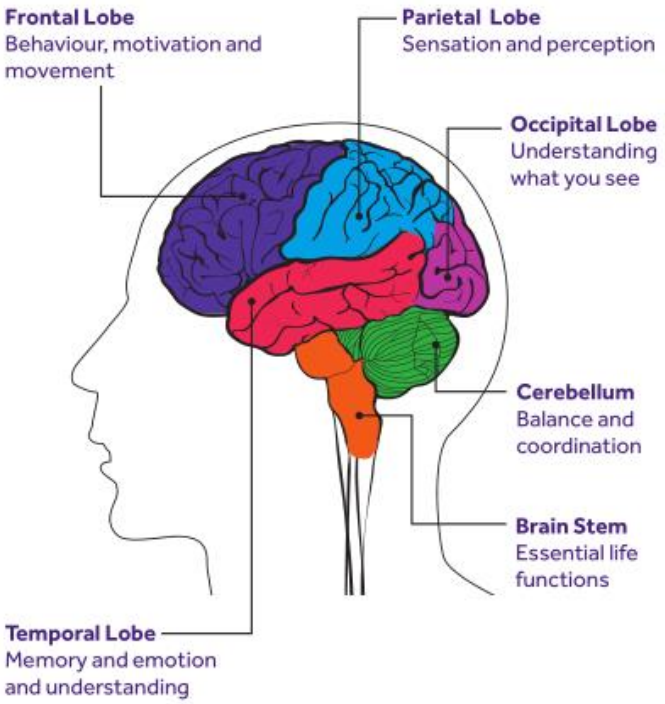

Figure 2.1: *Different regions of the brain associated with control of different behaviours (Stroke Association, 2018).*

Common symptoms include motor impairment along one side of the body (known as hemiparesis), paralysis along one side of the body (hemiplegia), impairment to speech (aphasia), difficulties swallowing, muscle spasticity (hypertonia) and impairment to memory. It was found in a study by Sommerfeld et al (2004) that up to 80% of Stroke patients initially experience motor difficulties. Lawrence et al (2001) performed a community-based study on

first-time Stroke patients and found that 77.4% of the Stroke patients suffered from upper limb impairment.

Stroke has a significant negative impact on a patient's quality of life. Regular activities such as walking, eating, and manipulating objects become difficult or impossible. This often leads to dependency on care and assistance from others. Aside from the personal impact on the patient, Stroke has financial implications for society. Xu et al (2018) estimated the mean cost of health and social care per Stroke patient to be £46,039. This figure is in close agreement with the Stroke Association (2017), who estimated that in 2015 the mean cost of health and social care per Stroke patient was £45,409.

2.1.2. Stroke Prevalence

A study by O'Mahony et al (1999) found that 1.75% of a sample population of 2000 had suffered from Stroke. Stroke can occur in people of any age, but it has been shown by the Stroke Association (2018) that the likelihood of an individual having a Stroke increases with age. According to the Office of National Statistics (2018) the population of the UK is aging, with 26.5% of the population projected to be aged 65 or older by 2041. This 'greying' of the population is common across most Western societies due to falling birth-rates and an increased life expectancy, a trend which is projected to become an issue globally. Figure 2.2 shows an age group distribution of the population using data gathered from 195 United Nations countries from 1950 onwards and projected to 2050 alongside a projection of the population aged 65 or older in the UK:

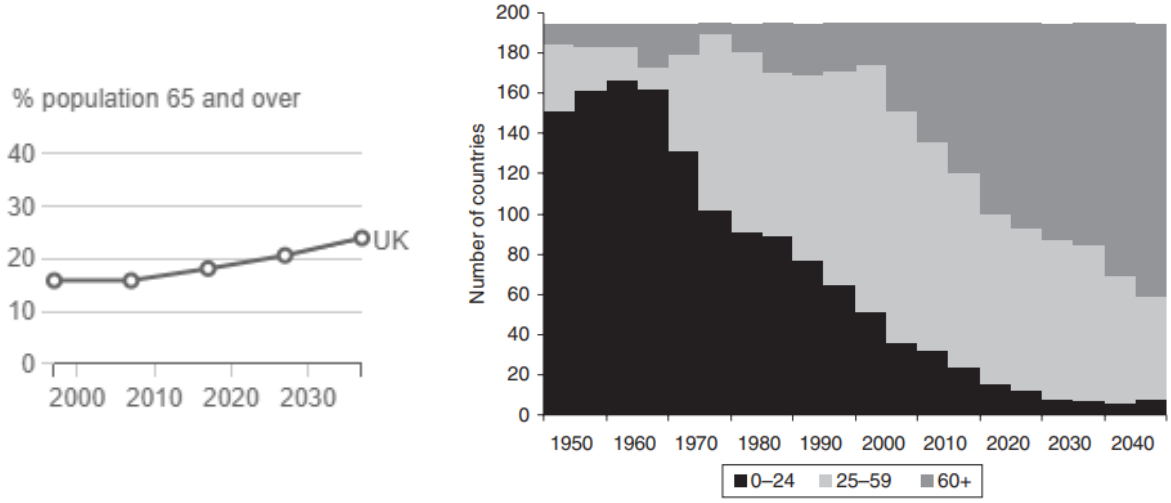

Figure 2.2: *Left: Aging population in the UK (Office of National Statistics, 2018), and Right: the world (Lee and Mason, 2011).*

Observing the projected trend, it is reasonable to expect that the total number of Strokes will increase. This will increase the demand and financial costs upon the NHS and rehabilitation services, especially when considering that the research shows that early and intensive physical rehabilitation is an important factor in recovery.

2.1.3. Neurological Recovery after Stroke

Since Stroke is a neurological issue, it follows that Stroke recovery must exploit neurological mechanisms. Cerebral plasticity (otherwise known as neurofunctional plasticity) is the ability of the brain to "reorganise during ontogeny, learning or following damage" (Duffau, 2006). It is this ability of the brain to reorganise that provides the mechanism for Stroke recovery, though this mechanism is not yet fully understood according to Kreisel et al (2007).

Without the intervention of rehabilitation, there does remain some natural motor recovery after Stroke, though this varies considerably from patient to patient. The timeline for natural motor recovery after Stroke is summarised in the table 2.1:

Stage		Timeline	Stroke Events	Plasticity
Onset			Stroke occurs	
Acute	**Hyperacute**	Up to 48hrs from onset	Consequences most prominent	
	Acute	Up to 4 days from onset	Secondary events reach full force	Most Dynamic
	Subacute	Anywhere from 48 hrs after onset, lasting 2-3 weeks	Secondary events begin to subside	Most Dynamic
Period of Consolidation		From end of Subacute phase, lasting no more than several months after onset		Dynamism slows
Chronic		Defined as the time after which the direct and secondary consequences have subsided and plastic process become static	All primary and secondary events subsided	Dynamism ends

Table 2.1: *Natural motor recovery after stroke.*

It can be seen from table 2.1 that the neurofunctional plasticity of the brain is most dynamic after the Hyperacute phase, but then the dynamism slows. Once the patient has reached the Chronic stage, the plastic processes become static and motor deficits remain unchanged after this point without the intervention of therapy (Kreisel et al, 2007).

2.1.4. Physiotherapy after Stroke

The use of physiotherapy is an accepted element for the rehabilitation of Stroke patients. Physiotherapy is applied by trained physiotherapists, though there has been a rise in the use of robots for post-Stroke physiotherapy in recent years. There is little agreement on the effectiveness of different rehabilitation strategies. Two main rehabilitation strategies are in widespread use according to Morreale et al (2016) and Coleman et al (2017). Proprioceptive Neuromuscular Facilitation (PNF) involves stretching and contracting a targeted muscle group, as shown by figure 2.3:

Figure 2.3: *Proprioceptive Neuromuscular Facilitation (PNF) (Marek et al, 2005).*

More advanced PNF involves resisting the movement of the patient, although this relies on the patient having enough motor control to move the exercised limb.

Cognitive Therapeutic Exercise (CTE) involves high level cognitive training through task-based activity (Lee et al, 2015). Robotic rehabilitation devices use the CTE strategy due to the ease of the gamification of tasks using computer game or virtual reality technologies.

Van Peppen et al (2004) performed a systematic review which showed that physical rehabilitation is more effective when performed intensively and early after Stroke. This is corroborated by Morreale et al (2016), who observed that early intervention was a factor on the effectiveness of rehabilitation. Indeed, these findings make sense when considering the neurofunctional plasticity of the brain is most dynamic early after onset, as shown in table 2.1. Morreale et al (2016) also stated, however, that "the optimal schedule and content of rehabilitation in the acute phase of care is still undefined". It is generally agreed that early intervention of physical rehabilitation is important for recovery, but there is little evidence to support the existence of an optimal rehabilitation strategy. Kreisel et al (2007) agree, stating that "mechanisms that support or modulate recovery are not yet fully understood".

2.2. Using Robots for Rehabilitation of Stroke Patients

In recent years there has been an increase in interest and research into the use of robots for rehabilitation of Stroke patients. According to Maciejasz et el (2014) and Culmer (2007), rehabilitation robots are categorised by their mechanical structure as either an end-effector based device or an exo-skeleton based device. These can be further categorised as Class 1 or Class 2 devices, as stated by Sulzer et al (2007) and Sivan et al (2014). Class 1

devices are of high cost and intended for lab or hospital use, whereas Class 2 devices are low cost and intended for home use. Most of the research in robotic rehabilitation devices has focused on Class 1 devices, since it was necessary to produce evidence that robotic rehabilitation was a valid rehabilitation strategy. However, Johnson et al (2007) identified a "need to improve the cost-to-benefit ratio of robot-assisted therapy strategies and their effectiveness for stroke therapy in home environments characterized by the low supervision by clinical experts, low extrinsic motivation as well as low cost requirement", which justifies further work in the area of Class 2 devices.

2.2.1. Control Hierarchy

An established control hierarchy exists for rehabilitation robotics, which is necessary since a high-level rehabilitation strategy must be encoded as low-level strategies according to Marchal-Crespo and Reinkensmeyer (2009). The high-level control strategy is responsible for generating tasks which fulfil rehabilitation aims. A trajectory must be generated from these tasks, and finally the low-level controller must use these trajectories to generate actuator demands. The low-level control strategies usually run in real time, since these control specific implementations of force, position or other types of interaction control. This hierarchy is shown by figure 2.4:

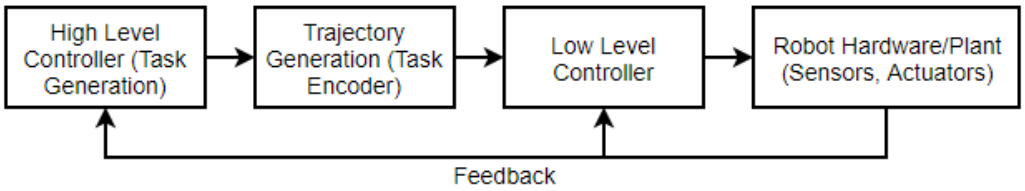

Figure 2.4: *Rehabilitation Robotics Control Hierarchy.*

2.2.2. High Level Control Strategies

All rehabilitation robotic devices must consider and implement both high-level control strategies and low-level control algorithms according to both Maciejasz et al (2014), who performed a systematic review of rehabilitation robotic devices, and Marchal-Crespo and Reinkensmeyer (2009), who performed a systematic review of control strategies for rehabilitation robotic devices. The high-level control strategy describes the movement strategy of the robot designed to promote neurofunctional plasticity of the damaged motor control areas of the brain. Erol and Sarkar (2007) suggest that the role of the high-level controller is equivalent to the role of the physiotherapist, in that it monitors the status of the task, monitors the safety of the patient and "informs the low-level controller about the task updates".

High-level control strategies can be broadly split into four categories: 1. Assistive control, 2. Challenge based control, 3. Haptic stimulation, and 4. Non-contacting coaching (Maciejasz et al, 2014) and (Marchal-Crespo and Reinkensmeyer, 2009).

Assistive control is a strategy whereby the patient is aided to complete the task. Usually, measures are put into place to allow the patient to move unrestricted as long as the correct trajectory is being followed. If there is deviation from the desired trajectory a restoring force proportional to the level of deviation is applied, as seen with the MIT-MANUS (Krebs et al, 2004). An Assistive control strategy is commonly implemented with Impedance or Admittance control as the low-level control algorithm. Another type of Assistive control uses a counterbalance to make a task easier for the patient, the Wilmington Robotic Exoskeleton (WREX) (Sanchez et al, 2005) being a good example. A further method of implementing Assistive control is to use Surface Electromyography (sEMG) sensors to measure signals in the nerves which are used to trigger assistance according to the patient's movement intention. This is difficult, however, since the noise to signal ratio is very high.

Challenge based control methods are designed to make the task more difficult for the patient, and are categorised as resistive, error amplifying or constraint induced. Resistive strategies resist the movement of the patient, simulating the more advanced techniques of Proprioceptive Neuromuscular Facilitation (PNF). Error amplifying strategies amplify movement errors rather than decrease them, according to Marchal-Crespo and Reinkensmeyer (2009). Error amplification strategies have been shown to increase motor learning compared with assistive strategies according to Patton et al (2006), who tested 18 hemiparetic Stroke patients.

Constraint induced strategies involve constraining the unimpaired limb, so that the impaired limb must perform the task. This particular strategy is particularly suited to exercises involving 2 limbs, for example reaching for a sizable object. Constraint induced strategies are not relevant, however, for end effector type devices such as the MIT-MANUS or MyPAM. In general, challenge-based control methods are not useful for severely impaired patients with little or no motor control, since the patient does not have sufficient control to begin the required movement.

Haptic strategies involve the use of Virtual Reality (VR) or Altered Reality (AR), where the user must where a headpiece which provides visual feedback in a 3-Dimensional environment. This was implemented by Montagne et el (2007), who found that the use of an engaging VR environment for visual feedback coupled with an exoskeleton robotic rehabilitation device significantly increased patient motivation. A clinical trial of this device showed increased motor control after 6 weeks of use, though only 3 chronic patients were tested and there is no evidence to show that the implementation of VR provides a greater clinical benefit than simply displaying visual feedback via a computer screen, as

implemented by many other robotic rehabilitation devices.

Non-contact coaching devices do not interact with the patient, and simply provide instructions to the patient, according to both Maciejasz et al (2014) and Marchal-Crespo and Reinkensmeyer (2009). This strategy may be useful for patients with high amounts of motor control but is not useful for patients with higher levels of disability who require assistance to complete exercises.

2.2.3. Trajectory Generation

As with any robot designed to move an end-effector from a starting position to a desired position, a trajectory must be generated. A number of approaches exist, the selection of which depends on what the trajectory is required to optimise. The simplest solution is to generate a simple linear trajectory which covers the shortest distance between the current position and the desired position, which is the current trajectory generation method for the MyPAM as shown in section 1.2.2 of this report. This method, however, potentially means that unacceptable changes in acceleration may be planned.

A better solution, implemented by the MIT-MANUS (Hogan et el, 1998), produces a Minimum Jerk Trajectory. A Minimum Jerk Trajectory minimises jerk, the third time derivative of position ($\frac{d^3x}{dt^3}$), which ensures that there should be no unacceptable changes in acceleration. Minimum Jerk Trajectories are an example of trajectories based on normative mathematics, which cover the most common trajectories used for rehabilitation robotics according to Marchal-Crespo and Reinkensmeyer (2009), though there is no evidence that normative trajectories maximise motor plasticity. Another common approach is to pre-record a trajectory, whilst a further, less common, method is to generate the trajectory based on the movement of the non-affected limb

2.2.4. Low-Level Control

It is the responsibility of the low-level controller to generate actuator demands according to the provided trajectory. This may be achieved simply by position control, as with the MyPAM, or Force control. More complex low-level controllers employ interaction control schemes. Maciejasz et al (2014) argue that the case of a robotic physiotherapy device interacting with a human patient should be considered as a coupled mechanical system. This means that the use of a force control strategy or a position control strategy alone is insufficient, since interaction forces with the patient are not accounted for and are thus inherently unsafe. Further to this, failure to account for interaction forces raises the possibility of controller instability. Hogan and Buerger (2004) demonstrated this instability by showing that the Rough-Hurwitz stability criterion were met when considering an example system in isolation but were not met when considering the same system in a coupled mechanism.

In order to account for interaction forces, the majority of rehabilitation robotic devices employ Impedance Control or Admittance Control as the low-level control strategy. Impedance Control and Admittance Control involve modulating the dynamic behaviour of the robot alongside position or force control, according to Hogan (1984), by specifying the robot's position and force relationship using virtual mass, spring and damping characteristics. Essentially, the desired position changes due to the application of an external force in a predictable manner defined by the mass, spring and damping characteristics, which are heuristically determined (Richardson, 2001). This is shown by figure 2.5:

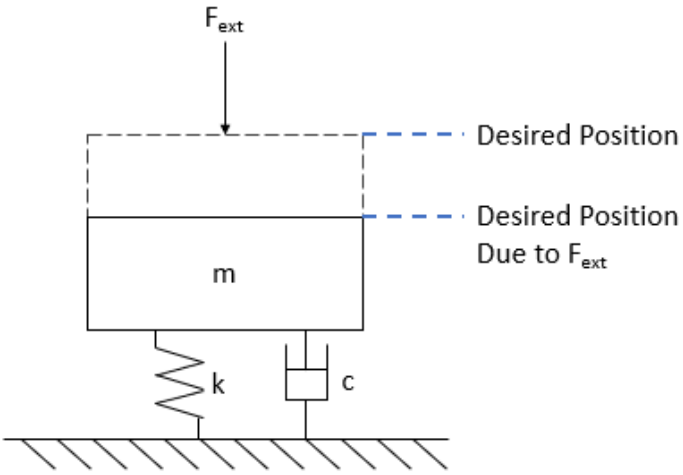

Figure 2.5: *The external force changing the desired position (Richardson, 2001).*

A physical system which accepts force inputs and produces position outputs is defined as an Admittance. A physical system which accepts position inputs and produces force outputs is defined as an Impedance (Ott et al, 2010) (Hogan,1984). The end effector of a mechanically coupled robot is subject to physical constraints, in such a way that it may act as either an Admittance or an Impedance. If the environment acts as an Admittance, the end effector must act as an Impedance according to Hogan (1984). Conversely, if the environment acts as an Impedance, the end effector must act as an Admittance. The practicalities of implementing this is discussed in the next 3 sections.

2.2.5. Admittance Control

Admittance control is a strategy where the force exerted on the end effector is measured, and the robot provides the corresponding displacement (Maciejasz et el, 2014). This means that the controller is acting as an Admittance and the environment is acting as an Impedance. As such, an Admittance control strategy is based around an inner loop position controller, as shown by the block diagram in figure 2.6:

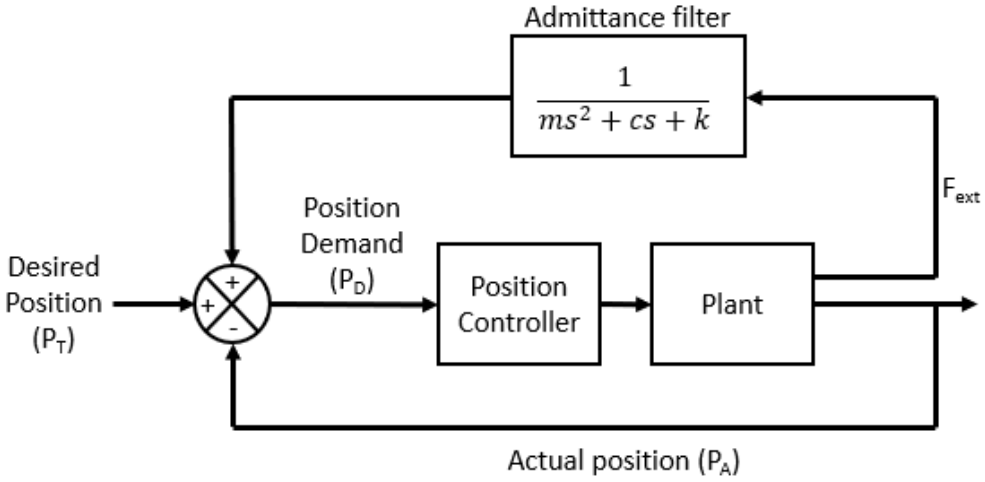

Figure 2.6: *A block diagram for a generic Admittance Controller (Richardson, 2001).*

According to Culmer et al (2010), the control signal can be simply defined as shown by equation 2.1:

$$P_D = P_t + \frac{F_{ext}}{ms^2 + cs + k} \qquad (2.1)$$

Where $\mathrm{P_D}$ is the position demand, $\mathrm{P_t} = P_T - P_A$ is the initial trajectory and $\mathrm{F_{ext}}$ is the interface force error.

This means that the interaction force error is used to adjust the position demand of the robot, where there are 2 control goals applied in order of importance:

1. Minimise the interaction force error between the environment and the end effector. In the context of rehabilitation robotics, the patient can be considered as the environment and the desired interaction force is 0N).
2. Minimise the distance between the Desired Position and the Actual Position.

2.2.6. Impedance Control

Impedance control is a strategy whereby the motion of the end effector is measured, and the robot provides the corresponding force-feedback (Maciejasz et el, 2014). This means that the controller is acting as an Impedance and the environment is acting as an Admittance. Whilst this is a slightly less intuitive approach than Admittance control, it is equally valid as a method to regulate interaction forces. An Impedance control strategy is based around an inner loop force controller, as shown by the block diagram in figure 2.7:

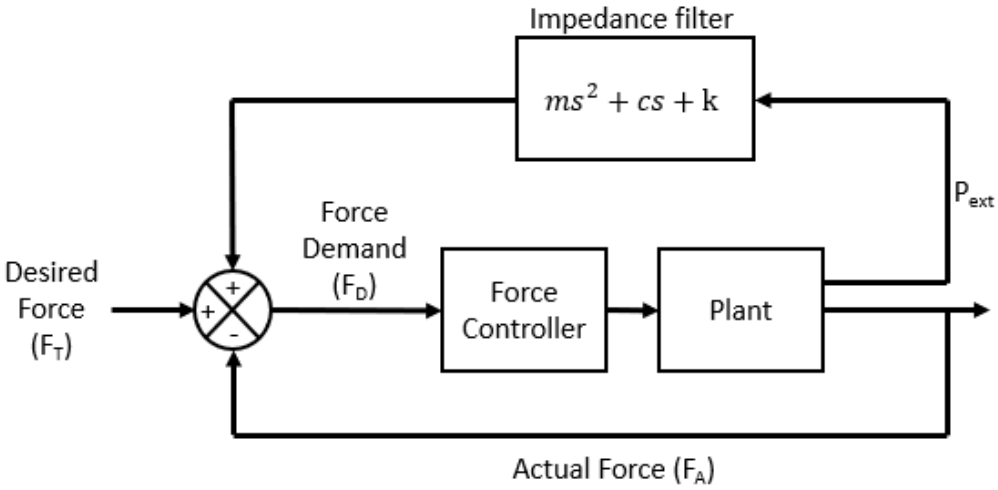

Figure 2.7: *A block diagram for a generic Impedance Controller (Richardson, 2001).*

According to Culmer et al (2010), the control signal can be simply defined as shown by equation 2.2:

$$F_D = F_t + P_{ext}(ms^2 + cs + k) \qquad (2.2)$$

Where $\mathrm{F_D}$ is the force demand, $\mathrm{F_t} = F_T - F_A$ is the initial force trajectory and $\mathrm{P_{ext}}$ is the position error.

This means that the position error is used to adjust the Force demand of the robot, where there are 2 control goals applied in order of importance:

1. Minimise the interaction position error of the robot, where an error in position is caused by the interaction force between the environment and the end effector.
2. Minimise the difference between the Desired Force and the Actual Force.

2.2.7. Selecting Impedance Control or Admittance Control

It is agreed by Ott et al (2010) and Maciejasz et el (2014) that the advantages and disadvantages of Impedance and Admittance control systems are opposite, which makes sense considering that the definition of a mechanical Impedance is the dual of the definition of a mechanical Admittance (Culmer, 2007). Devices using Impedance control are stable in stiff environments where there is resistance to motion but can be inaccurate in free environments due to unmodelled dynamics such as friction (Ott et al, 2010). Ott et al (2010) go on to state that devices using Admittance control provide “high level of accuracy in non-contact tasks but can result in instability during dynamic interaction with stiff environments”. This is corroborated by Maciejasz et el (2014) .

Anderson and Spong (1988) state the duality theory, which is that “the manipulator should be controlled to respond as the dual of the environment”. Simply put, this means that inertial environments, which act as an Impedance, require position based low-level control and the optimal interaction control strategy is Admittance control. In contrast, environments

characterised by a mass, spring and damper relationship, which act as an Admittance, require force based low-level control and the optimal interaction control strategy is Impedance control. In rehabilitation robotics the environment can be difficult to identify, and indeed can change dependent on patient capabilities. For example, a highly capable patient with a good level of motor control may be seen as an inertial environment, or Impedance, and thus is most suited to Admittance Control, whereas a patient with a high level of spasticity may be seen as a stiff environment, or Admittance, and thus is most suited to Impedance Control.

However, these criteria are not the sole determining factor on the most appropriate low-level control strategy. For example, whilst a robot actuated by direct drive electric motor systems may lend itself to force control (and thus Impedance control as an interaction control strategy), in reality this relies on an accurate dynamic model which can be difficult to obtain. Further to this, the robot would require force sensors at each joint, whereas a robot using Admittance control would require a force sensor only at the end effector, thus proving to be a more cost-effective solution. A comparison of Admittance control and Impedance control are summarised in table 2.2:

	Admittance Control	**Impedance Control**
Advantages	Only requires a force sensor at the end effector	Lends itself to direct drive electric motors, which are easy to move by torque control
	Does not require an accurate dynamic model	
Disadvantages	Requires a robust position control inner loop	Requires an accurate dynamic model to ensure controller stability
		Requires a force/torque sensor at each joint

Table 2.2: *Comparison of Interaction Control Techniques (Richardson et al, 2003).*

2.3. Rehabilitation Robots

Over the last 30 years, much work has been done in the area of rehabilitation robotics. In this section of the Literature Review there follows a brief overview of a selection of devices designed for upper limb rehabilitation of Stroke patients.

2.3.1. MIT-MANUS

MIT-MANUS was the first robotic device designed for the rehabilitation of upper limbs of Stroke patients. The device consists of a direct-drive five bar-linkage SCARA (Selective Compliance Assembly Robot Arm) which provides 2 DoF movement for the elbow and forearm in the horizontal plane (Krebs et al, 2004). MIT-MANUS guides the patient's arm through a series of predetermined exercises, with visual feedback provided on a computer screen according to Hogan et al (1995).

A series of extension devices were designed to aid in rehabilitation, since trials of MIT-MANUS found that positive motor learning effects on the exercised muscle groups did not have any effect on unexercised muscle groups. The first module extends the operating range of the MIT-MANUS by adding a third degree of freedom, which allow exercises to be performed in 3D space (Krebs et al, 2004). The second module was designed to rehabilitate the muscle groups in the hand. The MIT-MANUS and the hand module were successful enough that commercial products were released as the InMOTION Arm™ and the InMOTION Hand™. Figure 2.8 shows the InMOTION Arm™:

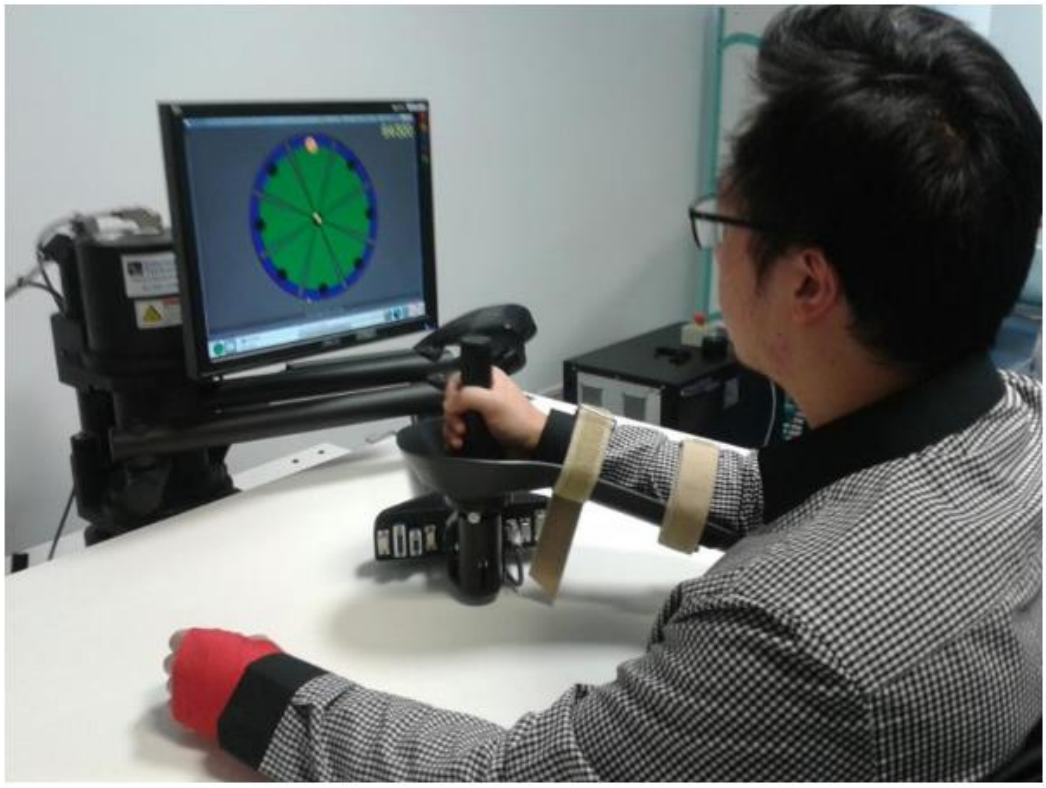

Figure 2.8: *The InMOTION Arm™.*

According to Krebs et al (2004), one of the driving design features for the MIT-MANUS is that it is "configured for safe, stable, and compliant operation in close physical contact with humans". This was achieved using Impedance Control as the low-level control strategy and ensuring that the hardware was backdrivable enough that frail patients could easily move the device. The Control hierarchy, which is similar that that seen across all robotic rehabilitation devices and defined in section 2.4.1, is shown by figure 2.9:

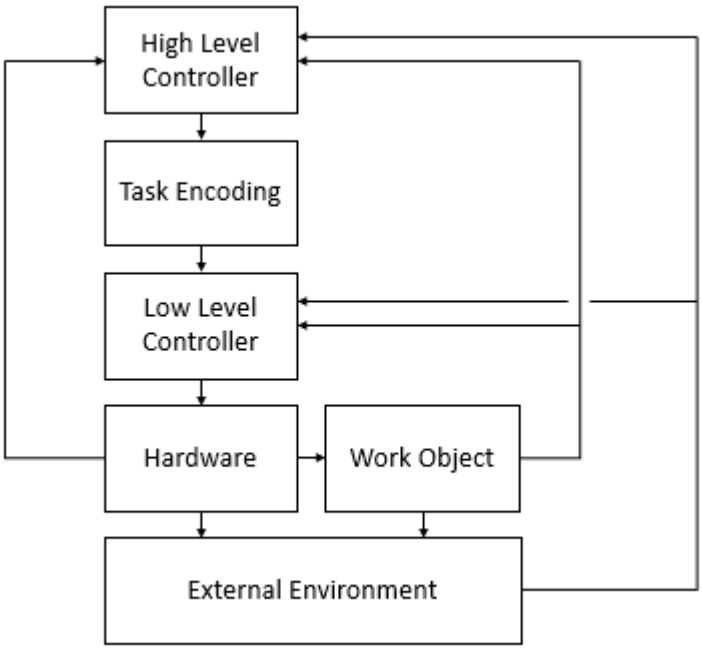

Figure 2.9: *The Control hierarchy for MIT-MANUS (Hogan et el, 1998).*

The hierarchy in figure 2.9 shows the following process:

1. A high-level controller sets the sequence of targets for the therapy session.
2. The Task encoder translates the sequence of targets into sets of Minimum Jerk Trajectories.
3. The low-level controller uses an Impedance control strategy which uses the trajectories to provide varying assistance levels to the patient and control the interaction forces.
4. Force and position feedback from the hardware and environment are used as feedback parameters.

MIT-MANUS has been subject to extensive clinical tests. An initial pilot study was performed in which half of a cohort of 20 patients, as the control group, received only physiotherapist guided therapy and the second half of the cohort, as the experimental group, received physiotherapist guided therapy alongside robot guided therapy. The results of the pilot trial showed that the patients who received robot led therapy alongside physiotherapist led therapy gained significant motor control in the targeted muscle groups (Krebs et al, 1998). Importantly, it was also found that patients in the experimental group improved "further and faster" than those in the control group (Krebs et al, 1998). A further study retested a subset of the patients 3 years after the initial therapy, and it was found that the experimental group "showed further significant decreases in impairment measures of the affected limb" (Volpe et al, 1999).

The InMOTION suite has recently undergone extensive trials, known as the Robot Assisted Training for the Upper Limb after Stroke (RATULS) trial, to determine whether robot-assisted training improved upper limb function compared with both normal post-Stroke care and a program of enhanced upper limb training (Rodgers et al, 2019). The study consisted of three groups. The first test group were assigned to robot assisted training using the InMOTION suite and 223 people in this group completed the study. The second test group were assigned enhanced upper limb therapy and 222 people in this group completed the study. The control group were assigned to usual care and 190 people in this group completed the study. The two test groups received 45 mins of therapy 3 times a week for a period of 12 weeks alongside the usual care provided by the NHS. The control group received the no more than the usual care provided by the NHS. Progress assessments were performed by each participant after the trial was complete, and then 3 months after and 6 months after the trial.

It was found that the use of robot-assisted training did not improve upper limb function after Stroke compared with enhanced upper limb training or normal care. Robot assisted training led to improvement in upper limb impairment compared with normal care but was not cost effective. Essentially, patients who received robot-assisted therapy were still disabled, but less impaired than patients who received normal care only. Robot-assisted training had a mean cost of £5387 per patient compared with the normal care cost of £3785 per patient (Rodgers et al, 2019).

2.3.2. MEMOS (Mechatronic System for Motor Recovery After Stroke)

The Mechatronic System for Motor Recovery After Stroke (MEMOS) is a 2DoF planar robotic rehabilitation system designed to be as low cost as possible. This was achieved by building the device using as many ‘off the shelf’ parts as possible and ensuring that any part which could not be simply bought was able to be manufactured as simply as possible (Micera et al, 2005), similar to the approach taken during the development of the MyPAM. Much like the MIT-MANUS, the MEMOS system guides the patient’s arm through a series of exercises with visual feedback provided on a computer screen.

The result of these cost saving measures is that the device costs only €4,450. This is considerably more cost effective compared with the estimated $100,000 for the InMOTION Arm™, which is also a 2DoF planar robot. The MEMOS system consists of a handle connected to a trolley which runs on rails in a cartesian configuration, shown by figure 2.10:

Figure 2.10: *The MEMOS system (Micera et al, 2005).*

The MEMOS system uses 3 High-level control strategies: Completely assisted movement where the patient provides no input, assisted movement where the patient provides some input, and unassisted movement where the patient provides total input. If the patient fails to produce a minimum force after a certain amount of time, the robot moves the handle to the target with a predefined velocity. This is clearly seen in the control signal shown by equation 2.3 (Micera et al, 2005):

$$s(t) = k_p F_p + V_R t \delta(F_{min}, T_D) \qquad (2.3)$$

Where $\mathrm{k_p}$ is the Admittance filter, $\mathrm{F_p}$ is the interaction force, $\mathrm{V_R}$ is the maximum assistance velocity, $\mathrm{F_{min}}$ is the minimum force threshold, $\mathrm{T_D}$ is the time threshold and $\delta(\mathrm{F_{min}}, \mathrm{T_D})$ is the function used to enable assistance.

It can be seen from the control signal that the low-level control strategy implemented is Admittance Control using a simple spring model only, although this choice is not explained.

MEMOS was subjected to a preliminary clinical trial containing 8 patients suffering from chronic hemiparesis after Stroke. The subjects' hemiparesis in all 8 subjects was considered to be only slightly to moderately impairing. The testing consisted of a 40-minute session with the device twice a day for 3 weeks, where the exercises consisted of reaching tasks (Micera et al, 2005). The results showed that 7 of the 8 subjects improved in motor control of the targeted muscles groups. Importantly, the results of the clinical trial showed that it is possible for rehabilitation to have an effect even in the chronic phase, although it should be noted that none of the tested subjects had severe impairment, so it is not possible to extrapolate the findings to severely disabled chronic Stroke patients. Indeed, it was noted that the MEMOS device would be best suited for use further down the rehabilitation process for home use and was no substitute for the more complex Class 1 devices available.

2.3.3. Mirror Image Motor Enabler (MIME)

After an initial 2-DoF prototype was built, the second iteration of the Mirror Image Motor Enabler (MIME) system used an industrial PUMA 6-DoF robot to move the impaired limb of a Stroke patient. The MIME device moves the patient's arm in a planar motion, with the weight of the arm borne by a separate support containing position sensors. The unaffected arm is connected to a separate support, also containing position sensors. A third iteration of the device used a larger PUMA 6 DoF robot which could support the full weight of the impaired limb and allow the separate support to be removed. The benefit of this was that a 3D workspace could be utilised. This arrangement is shown by figure 2.11:

Figure 2.11: *The 3rd iteration of the MIME system (Burgar et al, 2000).*

The MIME system has 4 high-level control strategies. The first is a completely assisted mode (in the literature called 'passive-guided mode'), where the robot moves the impaired limb along a predefined trajectory and the patient is required to input no effort. The second is an assisted mode, where the patient initiates movement of the impaired limb and the MIME robot provides assistance to complete the exercise. The third is a resistive mode, where the patient moves the impaired limb and the MIME robot resists the motion. The fourth is a novel bilateral mode, where the robot moves the impaired limb as a mirror image to the movement of the unimpaired arm, in a master/slave relationship (Lum et al, 2006).

There is no explicit description of the low-level control system, but the literature states that both joint position and patient-handle interaction force were measured (Lum et al, 2005), which suggests the use of an Admittance control scheme.

The MIME system has undergone extensive clinical trials. In an initial trial of the 3rd iteration of the device 11 chronic subjects were exposed to robot training therapy as the test group and 10 chronic subjects received traditional physiotherapy as the control group.

Therapy sessions lasted for 1 hour, and this occurred for 24 sessions over a 2-month period (Burgar et al, 2000). It was found that the robot test group experienced increased motor control in the targeted muscles groups to a greater extent than the control group, though at a 6 month follow up it was found that the gains were equivalent in both the test group and the control group.

In a further study subacute subjects were split into 4 test groups. The first of the groups were exposed to robot therapy that started as completely assisted and progressed into resistive therapy. The second of the groups were exposed to bilateral robot therapy. The third of the groups were exposed to robot therapy that was split between bilateral training and unilateral training. The fourth group were exposed to no robot therapy, but instead received an equal amount of traditional physiotherapy (Lum et al, 2005). The therapy sessions lasted for 1 hour, and this occurred 15 times over a 4-week period. The robot test groups demonstrated significantly increased motor control in the targeted muscle groups at the end of the testing, to a much greater extent than the control group. This is consistent with the previous study. However, at a 6 month follow up it was found that "gains in robot and control groups were equivalent" (Lum et al, 2005), similar to the chronic test group from the previous study.

In a follow up Lum et al (2006) suggest that from a pragmatic point of view, robotic therapy is useful for patient motivation when access to a physiotherapist may be limited, even if the long-term gains from robotic therapy are equivalent to that of traditional physiotherapy. To this end, it is suggested that research efforts should be directed towards producing low-cost versions of clinically tested robots.

2.3.4. Assisted Rehabilitation and Measurement (ARM) Guide

The Assisted Rehabilitation and Measurement (ARM) Guide is a 2 DoF device designed to rehabilitate and measure upper limb reaching movements of Stroke patients. The device is mechanically simple and consists of a splint connected to a linear slide rail. The splint is driven along the rail using an electric motor. The slide mechanism can be adjusted in the horizontal and vertical planes, allowing a variety of reaching exercises to be performed (Reinkensmeyer, 2001). The interaction force between the patient and the ARM Guide is measured using a 6 DoF force sensor. The ARM Guide is shown by figure 2.12:

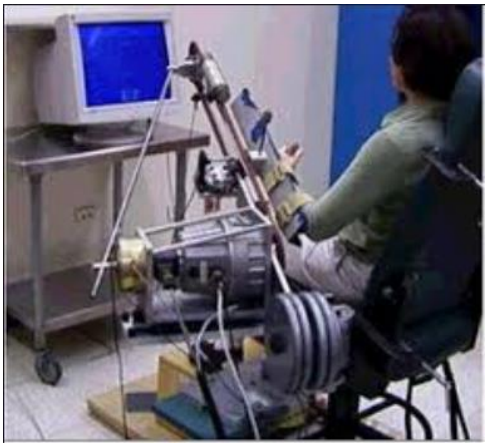

Figure 2.12: *The ARM Guide system (Reinkensmeyer et al, 2001).*

The ARM Guide system uses 2 distinct high-level control strategies. Due to the linear mechanical design of the ARM Guide system, all exercise trajectories are linear. The first high-level strategy is termed ‘Counterpoise Assistance’, which is based on traditional physiotherapy techniques. Counterpoise Assistance provides enough assistance to overcome passive forces resisting the desired motion, such as gravity and arm tone according to Reinkensmeyer et al (2001). The low-level control scheme which is implemented to achieve this involves measuring the resistive forces and counteracting them by applying an opposite force with the motor.

The second high-level strategy is Triggered Assistance, where full assistance is given to complete the reaching exercises as soon as the patient initiates the movement. The low-level control scheme uses a PD position control loop (Reinkensmeyer et al, 2001).

The ARM Guide was subjected to trials containing 19 Chronic Stroke patients suffering from hemiparesis, who were split randomly into 2 groups. The test group engaged in robot assisted reaching exercises and the control group engaged in unconstrained and unassisted reaching exercises. The study consisted of 24 separate sessions lasting 45 minutes over a period of 8 weeks. It was found that both groups had a significantly improved range of movement and velocity control at the end of the study, and that the robot assisted test group did not experience statistically significant detectable improvements in motor control beyond that experienced by the unassisted control group (Kahn et al, 2006).

2.3.5. End Effector Upper Limb Rehabilitation Robot (EEULRebot)

The End Effector Upper Limb Rehabilitation Robot (EEULRebot) is a planar system designed to assist in the rehabilitation of Stroke patients with upper limb motor control deficiencies. The planar workspace is adjustable in the vertical direction by adjusting the inclination angle, making the device quasi-3 DoF. The 2 joints are powered using Maxon motors. The end effector contains a force sensor to measure the interaction force between

the patient and the EEULRebot device. A SolidWorks model of this arrangement is shown by figure 2.13:

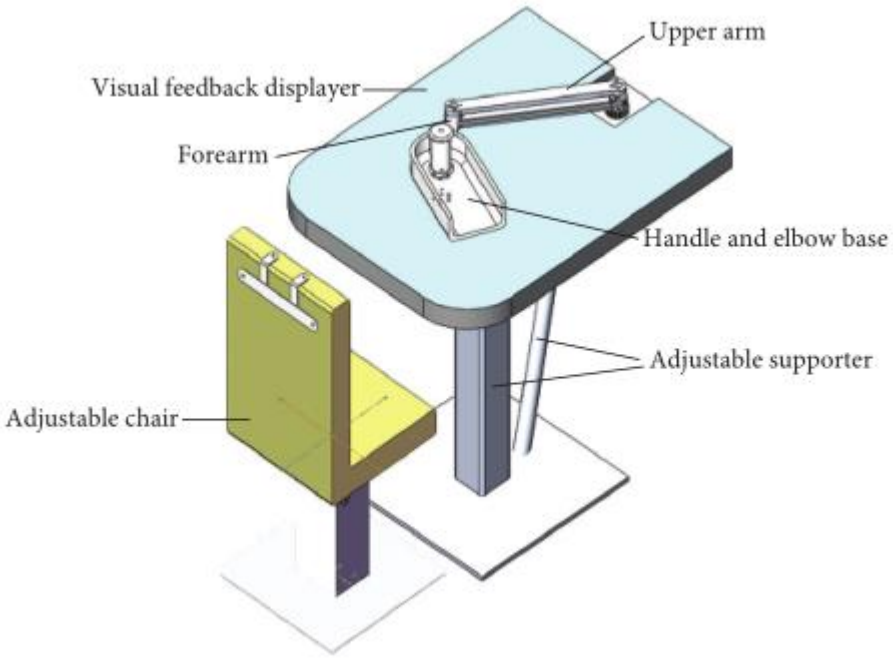

Figure 2.13: *A SolidWorks model of EEULRebot System (Liu et al, 2017).*

The EEULRebot System has 3 distinct high-level control strategies (Liu et al, 2017). Similar to the MIME System in section 2.3.3, The first is a completely assisted mode (in the literature called 'passive-guided mode'), where the robot moves the impaired limb along a predefined trajectory and the patient is required to input no effort. The second is an Assistive mode (in the literature called 'Active-Constrained mode') where the robot provides assistance to complete the exercise, and in particular provides a restoring force to ensure that any deviation from the desired trajectory is corrected. The third is a Resistive mode (in the literature called Active Assistant or Resistant Mode') where the robot resists the movement of the end effector if the user exceeds a velocity threshold in the direction of the desired trajectory, thus making the exercise more difficult.

Impedance control was used as the low-level control strategy, with a restoring force normal to the trajectory designed to align the current position with the current point on the desired trajectory (Liu et al, 2017). A force parallel to the direction of the desired trajectory was also defined. In the assistive mode this force was positive, helping the patient to move the impaired limb along the desired trajectory. In the resistive mode this force was negative, making it more difficult to complete the exercise.

The EEULRebot device underwent trials with 11 healthy subjects and 3 hemiplegic subjects who had suffered from a Stroke. The healthy subjects tested all 3 of the high-level control strategies, but only 1 of the hemiplegic subjects was physically able to do so. The

other 2 hemiplegic patients had insufficient motor control to test the Assistive mode or the Resistive mode, and so only tested the Passive-guided mode. The trial was designed to test the robustness of the device rather than to validate it in as a useful clinical tool. The trials demonstrated that the EEULRebot was robust in that the control strategies worked as intended, though it was noted that further extensive trials were required with a greater number of impaired test subjects (Liu et al, 2017).

2.3.6. intelligent Pneumatic Arm Movement (iPAM)

The intelligent Pneumatic Arm Movement (iPAM) is a cooperative dual robot system designed for upper limb rehabilitation of Stroke patients. Each of the dual iPAM robots uses pneumatic actuators to power the movement of its 3 joints (Culmer et al, 2005). Similar to other rehabilitation robotic devices, iPAM guides the patient's arm through a series of exercises with visual feedback provided on a computer screen. The iPAM dual robot system is shown by figure 2.14:

Figure 2.14: *The iPAM system (Jackson et al, 2007).*

The iPAM uses Assistive control as the high-level control strategy, and so it assists the patient to complete the exercises. The input trajectory fed to the low-level control scheme is based on the kinematics of the arm. The high-level control strategy, task encoding and low-level control implementation procedure is consistent with the control hierarchy defined in section 2.4.1.

The iPAM uses Admittance control for the low-level control strategy. The control scheme is cooperative, since both robots must act in unison (Jackson et al, 2007). Admittance control was chosen because it favours pneumatic actuation, as agreed by Culmer (2010) and Richardson et al (2006). This is because it is difficult to model the non-

linear dynamic effects, such as stiction, of pneumatic actuators accurately enough to ensure the accuracy of the force control inner loop required for Impedance control. The level of assistance provided to the patient is changed by altering the stiffness coefficient in the Admittance filter.

Initial trials demonstrate that the iPAM is capable of providing assistance to the upper limb with similar trajectories and patterns of movement to a subject's unconstrained motion (Jackson et al, 2007). This was considered important because the system was designed not to exert unwanted and uncontrolled forces on the limb, which would encourage unnatural motions. It was noted, however, that the device was unsuitable for use with patients who had "little to no voluntary movement" (Jackson et al, 2007). It was necessary for the patient to have some amount of motor control because the device was not capable of providing total assistance.

2.3.7. hCAAR (home-based Computer Aided Arm Rehabilitation)

The hCAAR (home-based Computer Aided Arm Rehabilitation) system, the predecessor of the MyPAM, is a 2DoF planar device developed to be installed in the houses of Stroke patients for upper limb rehabilitation, as well as in community locations to aid in the rehabilitation of children with Cerebral Palsy. The aim of this Class 2 rehabilitation robot was to increase patient therapy hours, since literature suggests that the more access to therapy a patient has the greater the potential for neurofunctional motor recovery. The hCAAR system guides the patient's arm through a series of games, with visual feedback provided on a computer screen, as shown by figure 2.15:

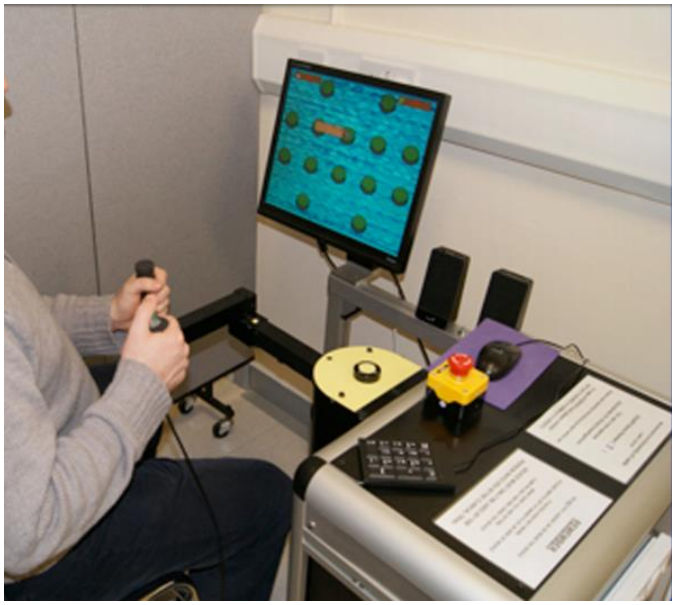

Figure 2.15: *The hCAAR system (Sivan et al, 2014).*

Since the hCAAR was intended for home use, it was designed to be as cost effective as possible. To this end, the first iteration of hCAAR used only PID position control as the

low-level control strategy to limit the use of expensive sensors. The second iteration of the hCAAR system used a novel form of Impedance Control as the low-level control strategy whereby the motor current draw at each joint motor were estimated from a system model, allowing an inner loop which controls motor current draw rather than directly controlling torque, according to Firouzy (2011). This means that expensive torque sensors were not required for the force feedback necessary for an inner force control loop. The downside to this is that current measurements are noisy and thus the reliability of the control system was questionable.

The hCAAR has 2 distinct operation modes, which can be considered as the high-level control strategies. The first mode is assistive where a variable level of assistance aids the patient to complete the tasks. The second mode is entirely passive and is used to collect data about patient progress.

The first iteration of the hCAAR system, which used PID position control only, was subjected to clinical trials with 19 patients, 17 of which completed the trial. Each patient had a hCAAR device installed in their home for a period of 8 weeks in order to undertake home exercises alongside their usual rehabilitation. A baseline assessment was carried out just before home installation, an assessment was carried out after the 8-week trial period and a further assessment was carried out after another 4 weeks (at the 12-week period). According to Sivan et al (2014), “statistically significant improvements were observed”, though it was noted that a study “comparing the combination of conventional therapy and hCAAR with conventional therapy alone needs to be explored”. It should be noted also that with position control only there is no mechanism for measuring or controlling the interaction forces with the patient, and thus dangerous torques or forces could occur.

2.3.8. RUPERT (Robotic assisted Upper Extremity Repetitive Therapy)

The Robotic assisted Upper Extremity Repetitive Therapy (RUPERT) device is an exoskeleton robot designed to rehabilitate Stroke patients suffering from upper limb mobility problems. The RUPERT device is aimed specifically at training 3DoF reaching tasks critical for daily living (Sugar et al, 2007). Assistance is provided to the patient through the use of pneumatic ‘air muscles’, much like the iPAM in section 2.5.6. The RUPERT system is shown in figure 2.16:

Figure 2.16: *The RUPERT system (Sugar et al, 2007).*

Common to many robotic rehabilitation devices, RUPERT uses Assistive control as the high-level control strategy. The patient is requested to make a movement. If after a certain amount of time the patient has been unable to do so, RUPERT provides assistance. Interestingly, the low-level control of the RUPERT device relies on open loop feedforward position control. This means that the physiotherapist must set and monitor speed and position parameters in order to ensure patient safety, along with a set limit on the maximum angular speed of the joints. Sugar et al (2007) acknowledge the limitations of this low-level control algorithm, stating that closed loop control would be required when dealing with more severely impaired patients.

The second iteration of the RUPERT device was subjected to limited clinical trials, which ran for 3 weeks, containing 10 Stroke patients who had moderate or mild upper limb motor control difficulties. Though the testing description is limited, 6 of the 10 test subjects completed the trials and 5 of these showed improvements in motor control in the targeted muscle groups.

2.4. Summary of the Literature

There has been much development in the use of robotics to provide rehabilitation for Stroke patients in recent years, which has been prompted by the financial and social implications of an aging population where Stroke is becoming increasingly prevalent. The area of robotic rehabilitation is dominated by 2 main classes of devices. The first is exoskeleton-based robotics, and the second is end-effector based devices. These can be further split into Class 1 devices, intended for clinical and lab use, and Class 2 devices, intended to be low cost and installed for home use.

Rehabilitation robotics devices follow an established control strategy. The high-level control strategy is designed to follow established physiotherapy principles which attempt to promote neurofunctional plasticity, though this area is not well understood. A trajectory is generated, and the low-level control strategy describes the specific implementation of position, force, Impedance or Admittance control.

Many of the devices utilise some form of interaction control for the low-level control strategy. Interaction control was heavily developed by Hogan and can take the form of Admittance control or Impedance control, though some rehabilitation robotics devices use a hybrid form of the two. The MIT-MANUS, for example, uses Impedance control and the iPAM uses Admittance control.

A literature review has identified research gaps. Johnson et al (2007) identified a requirement to develop low cost solutions for rehabilitation robotics, which is significant because the leading commercial solution, the InMOTION Arm™, costs in excess of $100,000. Marchal-Crespo and Reinkensmeyer (2009) suggest that future research efforts should focus on a “rigorous comparison of control algorithms” to determine whether there is any clinical benefit to the selection of one over another. There is evidence that the use of rehabilitation robotics can positively affect motor control of targeted muscle groups, but consistent with traditional physiotherapy, there is no consensus on an optimal high-level strategy, low-level implementation or rehabilitation schedule. This is because “mechanisms that support or modulate recovery are not yet fully understood” (Kreisel et al, 2007) .

The recent RATULS study found that the use of rehabilitation robotics in a clinical setting provided an improvement in upper limb impairment compared with normal care alone, but it was not cost effective. This supports the development of low-cost rehabilitation robotics for home use.

Chapter 3: Current Work

3.1. Trajectory Generation

As described in section 1.2.2, in the current version of the MyPAM the game generates equidistant intermediate positions between the start position and the final position of each reaching movement and passes these one at a time to the low-level controller. This leads to a number of issues:

1) A linear trajectory of this nature is not reflective of natural human motion, although there is no evidence that normative trajectories which mimic human motion promote neurofunctional plasticity (Marchal-Crespo and Reinkensmeyer, 2009).
2) The game does not operate at 30 Hz reliably as a result of being dependant of the non-deterministic Microsoft Windows Operating System (OS). There may be instances where the game rate will drop, resulting in incorrect intermediate position data being sent to the controller.
3) There are occasions where no intermediate points are generated and the final target position is sent to the controller as the next target, for example during some game types and during transitions between different games. This leads to a large difference between the current position and the target position, and large motor demands are generated. This leads to aggressive accelerations and potentially dangerous interaction forces between the patient and the robot.

3.1.1. Generating a Smooth Trajectory

A smooth trajectory is desirable when assisting the user to reach a target. This is because smooth trajectories are necessary to ensure safe interaction between the robot and the patient (Amirabdollahian et al, 2002) and movement smoothness is an indicator of increased motor control after stroke according to Balasubramanian et al (2015), though there is no evidence to suggest that assisting a smooth movement increases neurofunctional plasticity. Mathematically, a smooth trajectory translates to minimising the rate of change of an input, where the input corresponds to the order of the system. For example, a 1st order system corresponds to a kinematic model where velocities may be arbitrarily specified. This is summarised in the table 3.1 below:

Order of the system	Input to the system
1st	Velocity, $\dot{x}$
2nd	Acceleration, $\ddot{x}$
3rd	Jerk, $\dddot{x}$
4th	Snap, $x^{(4)}$
5th	Crackle, $x^{(5)}$
6th	Pop, $x^{(6)}$

Table 3.1: *Order of the system depends on the input to the system.*

The function for the trajectory may be found using Calculus of Variations, using the general equation shown by Equation 3.1:

$$x^*(t) = argmin_{x(t)} \int_0^T L\, dt \tag{3.1}$$

Where $L = \left(x^{(n)} \right)^2$.

Alternatively, the trajectory may be found by satisfying the Euler-Lagrange equation shown by Equation 3.2:

$$\frac{\partial L}{\partial x} - \frac{d}{dt}\left(\frac{\partial L}{\partial \dot{x}}\right) + \frac{d^2}{dx^2}\left(\frac{\partial L}{\partial \ddot{x}}\right) + \cdots + (-1)^n \frac{d^n}{dx^n}\left(\frac{\partial L}{\partial x^{(n)}}\right) = 0 \tag{3.2}$$

3.1.2. Minimum Jerk Trajectories

For a Minimum Jerk Trajectory, $L = (\dddot{x})^2$, since a minimum jerk trajectory is based on minimising the sum of squared jerk across the trajectory (Flash and Hogan,1985).
Forming the Euler-Lagrange formulation as shown by Equation 3.3:

$$\frac{\partial L}{\partial x} - \frac{d}{dt}\left(\frac{\partial L}{\partial \dot{x}}\right) + \frac{d^2}{dx^2}\left(\frac{\partial L}{\partial \ddot{x}}\right) - \frac{d^3}{dx^3}\left(\frac{\partial L}{\partial \dddot{x}}\right) = 0 \tag{3.3}$$

$$\frac{\partial L}{\partial x} = 0, \quad \frac{\partial L}{\partial \dot{x}} = 0, \quad \frac{\partial L}{\partial \ddot{x}} = 0, \quad \frac{\partial L}{\partial \dddot{x}} = 2\dddot{x} \tag{3.4}$$

$$-\frac{d^3}{dx^3}\left(\frac{\partial L}{\partial \dddot{x}}\right) = -\frac{d^3}{dx^3}(2\dddot{x}) = -2x^{(6)} = 0 \tag{3.5}$$

$$x^{(6)}(t) = 0 \tag{3.6}$$

$$x^{(5)}(t) = \int 0\, dt = c_5 \tag{3.7}$$

$$x^{(4)}(t) = \int x^{(5)}(t)\, dt = c_5 t + c_4 \tag{3.8}$$

$$\dddot{x}(t) = \int x^{(4)}(t)\, dt = c_5 t^2 + c_4 t + c_3 t \tag{3.9}$$

$$\ddot{x}(t) = \int \dddot{x}(t) dt = c_5 t^3 + c_4 t^2 + c_3 t + c_2 \tag{3.10}$$

$$\dot{x}(t) = \int \ddot{x}(t)\, dt = c_5 t^4 + c_4 t^3 + c_3 t^2 + c_2 t + c_1 \tag{3.11}$$

$$x(t) = \int \dot{x}(t) dt = c_5 t^5 + c_4 t^4 + c_3 t^3 + c_2 t^2 + c_1 t + c_0 \tag{3.12}$$

The boundary conditions are shown by table 3.2:

	Position, x	Velocity, $\dot{x}$	Acceleration, $\ddot{x}$
t = 0	a	0	0
$t = t_f$	b	0	0

Table 3.2: *Boundary conditions for a Minimum Jerk Trajectory.*

The function x(t) shown by Equation 3.12 must be differentiated twice to give the function for velocity and acceleration.

$$x(t) = c_5t^5 + c_4t^4 + c_3t^3 + c_2t^2 + c_1t + c_0 \quad (3.12)$$

Thus:

$$\dot{x}(t) = 5c_5t^4 + 4c_4t^3 + 3c_3t^2 + 2c_2t + c_1 \quad (3.13)$$

$$\ddot{x}(t) = 20c_5t^3 + 12c_4t^2 + 6c_3t + 2c_2 \quad (3.14)$$

Substituting boundary conditions:

$$x(0) = c_0 = a \quad (3.15)$$

$$x(t_f) = c_5{t_f}^5 + c_4{t_f}^4 + c_3{t_f}^3 + c_2{t_f}^2 + c_1t_f + c_0 = b \quad (3.16)$$

$$\dot{x}(0) = c_1 = 0 \quad (3.17)$$

$$\dot{x}(t_f) = 5c_5{t_f}^4 + 4c_4{t_f}^3 + 3c_3{t_f}^2 + 2c_2t_f + c_1 = 0 \quad (3.18)$$

$$\ddot{x}(t0) = c_2 = 0 \quad (3.19)$$

$$\ddot{x}(t_f) = 20c_5{t_f}^3 + 12c_4{t_f}^2 + 6c_3t_f + 2c_2 = 0 \quad (3.20)$$

Solving for the coefficients:

$$\begin{bmatrix} 0 & 0 & 0 & 0 & 0 & 1 \\ {t_f}^5 & {t_f}^4 & {t_f}^3 & {t_f}^2 & t_f & 1 \\ 0 & 0 & 0 & 0 & 1 & 0 \\ 5{t_f}^4 & 4{t_f}^3 & 3{t_f}^2 & 2t_f & 1 & 0 \\ 0 & 0 & 0 & 1 & 0 & 0 \\ 20{t_f}^3 & 12{t_f}^2 & 6t_f & 2 & 0 & 0 \end{bmatrix} \begin{bmatrix} c_5 \\ c_4 \\ c_3 \\ c_2 \\ c_1 \\ c_0 \end{bmatrix} = \begin{bmatrix} a \\ b \\ 0 \\ 0 \\ 0 \\ 0 \end{bmatrix} \quad (3.21)$$

$$\begin{bmatrix} c_5 \\ c_4 \\ c_3 \\ c_2 \\ c_1 \\ c_0 \end{bmatrix} = \begin{bmatrix} 6\left(\frac{b-a}{{t_f}^5}\right) \\ -15\left(\frac{b-a}{{t_f}^4}\right) \\ 10\left(\frac{b-a}{{t_f}^3}\right) \\ 0 \\ 0 \\ a \end{bmatrix} \quad (3.22)$$

Substituting the coefficients into equation 3.12 produces equation 3.23:

$$x(t) = 6\left(\frac{b-a}{{t_f}^5}\right)t^5 - 15\left(\frac{b-a}{{t_f}^4}\right)t^4 + 10\left(\frac{b-a}{{t_f}^3}\right)t^3 + a \quad (3.23)$$

Finally producing the minimum jerk trajectory shown by equation 3.24:

$$x(t) = x_i + (x_f - x_i)\left(6\left(\frac{t}{t_f}\right)^5 - 15\left(\frac{t}{t_f}\right)^4 + 10\left(\frac{t}{t_f}\right)^3\right) \quad (3.24)$$

Where x_i is the initial starting position, x_f is the target position, t_f is the target time from start and t is the current time.

This matches the function for a Minimum Jerk Trajectory found by Flash and Hogan (1985). A similar proof by Calculus of Variations may be found in Appendix A.

3.1.3. Justifying the use of a Minimum Jerk Trajectory

A Minimum Jerk Trajectory produces a smooth trajectory, but so too do other trajectories based on minimising the squared sum of derivatives of position. Figure 3.1 shows position and velocity graphs for the Minimum Acceleration, Minimum Jerk, Minimum Snap, Minimum Crackle and Minimum Pop trajectories to displace x from 0-100mm in 2 seconds. It may be observed that as the order of the system increases the position curve approaches a step function and the peak acceleration increases.

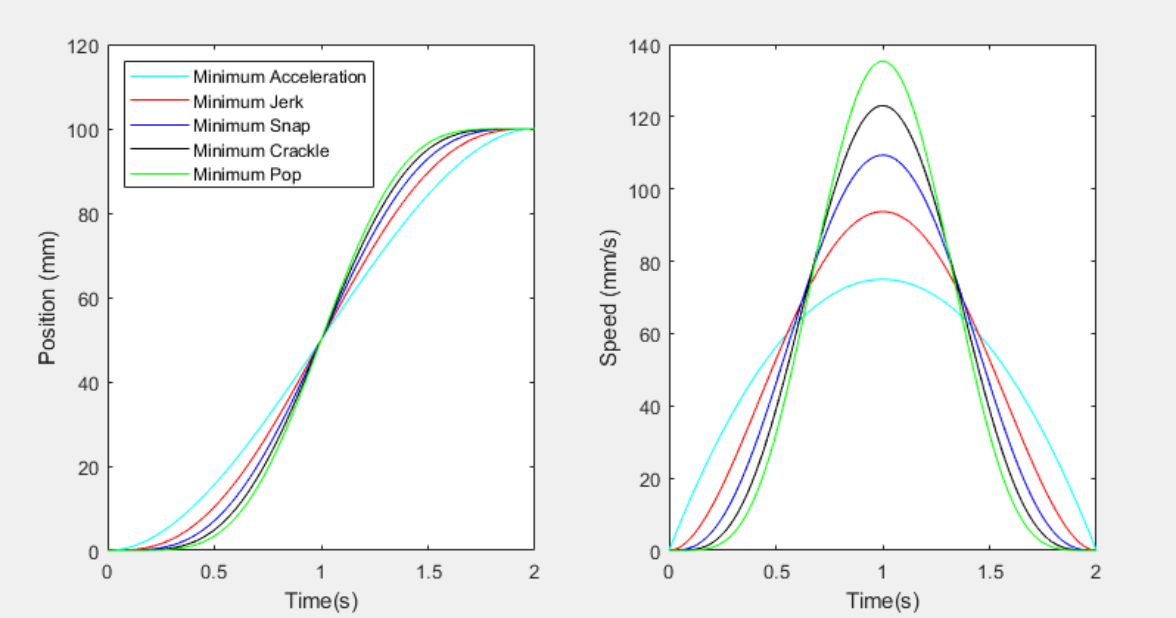

Figure 3.1: *Position and Velocity Graphs showing a displacement of 100mm in 2 seconds using Minimum Acceleration, Jerk, Snap, Crackle and Pop trajectories.*

For assistive rehabilitation technology, it may potentially be advantageous to generate a trajectory which mimics human movement, though there is no evidence to support this. According to Richardson and Flash (2002), one measure of human reaching motion is the ratio of peak velocity to average velocity across the movement. Flash and Hogan (1985) found that the ratio of peak velocity to average velocity, *R*, across a reaching movement is around 1.8. The ratio for Minimum Acceleration, Minimum Jerk, Minimum Snap, Minimum Crackle and Minimum Pop trajectories is shown by table 3.3:

Trajectory Type	R = Peak Velocity/Average Velocity
Minimum Acceleration	1.50
Minimum Jerk	1.88
Minimum Snap	2.19
Minimum Crackle	2.46
Minimum Pop	2.71

Table 3.3: *The ratio of peak velocity to average velocity given by different trajectory types.*

Thus, it is clear that by this measure the Minimum Jerk trajectory most closely resembles natural human motion and is therefore the most appropriate trajectory for the MyPAM.

3.2. End-Effector Force Sensor

A necessary component for Admittance control and Impedance control is the ability to measure the interaction force between the patient and the end effector. Since the MyPAM is planar, it is only necessary to measure the global X and Y components of force. The majority of rehabilitation robots which require a force sensor use off-the-shelf force sensors. For example, the iPAM used a 6-axis ATI Mini40 (Culmer, 2007), with a cost of around $5500. Since the MyPAM is designed to be a low-cost device it is necessary to develop an economically viable force sensor.

The majority of industrial force sensors operate by measuring strain and converting this into a force reading. Other force sensing methodologies include piezoelectric transducers. Both of these methodologies have downsides. Strain based force measurements require considerable signal processing and are susceptible to measurement noise. The signal conditioning required is difficult and can add significant cost. Piezoelectric transducers are susceptible to drift, especially when exposed to prolonged force. In recent years there has been much development in low-cost tactile sensors which use strong magnets offset from Hall Effects sensors by hyperelastic silicon material (Wang et al, 2016). This is promising because it allows a low-cost force sensor to be designed for the MyPAM.

3.2.1. Sensor Design

The handle for the end effector and 2 DoF force sensor were designed as an integrated unit. A rigid aluminium core, which connects to the end effector housing, was embedded with 4 Hall Effect sensors. A rigid outer core embedded with neodymium magnets was placed round the inner core, and a hyperelastic silicon material separation layer was placed between the 2 cores, such that an applied force allows the outer core to displace relative to the inner core. This arrangement is shown by figure 3.2:

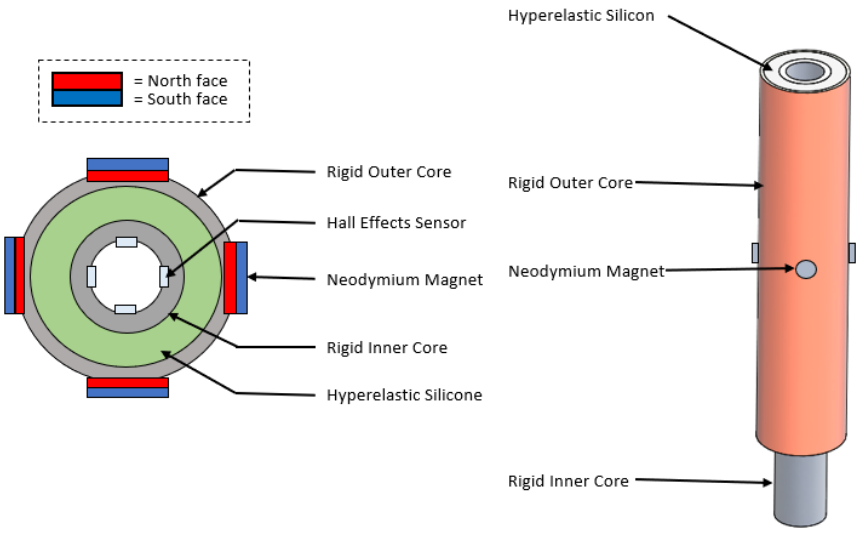

Figure 3.2: *The integrated end-effector and force sensor design.*

EcoFlex™ 0010 and EcoFlex™ 0050 were selected as the hyperelastic silicon material separation layer because materials from EcoFlex™ have successfully been used in the manufacture of low-cost force sensors previously by Wang et al (2016). Finite Element Analysis (FEA) was performed to determine the optimum configuration for the hyperelastic silicon separation layer. There were difficulties in modelling the hyperelastic silicon however, since the EcoFlex™ products are not traditional engineering materials and as such do not have published material properties. Further to this, whilst EcoFlex™ products have been used in a similar manner in some published scientific work, either the necessary material properties have either been left unpublished or there is significant disagreement in the published data, which may have arisen due to differences in mixing ratios and testing environments. To this end the FEA results were not considered reliable and 4 physical prototypes were built to find the most appropriate composition. It should be noted that EcoFlex™ 0010 is significantly softer, elastic, and more compliant than EcoFlex™ 0050.

Test piece *i* used EcoFlex™ 0010 which was cast 20mm form each end of the test piece, leaving a void throughout the centre of the test piece. Test piece *ii* was similar to test piece *i*, but used EcoFlex™ 0050. Test piece *iii* used EcoFlex™ 0010 cast throughout the entire length of the test piece. Test piece *iv* used EcoFlex™ 0050 cast throughout the entire length of the test piece. This can be seen in figure 3.3 below:

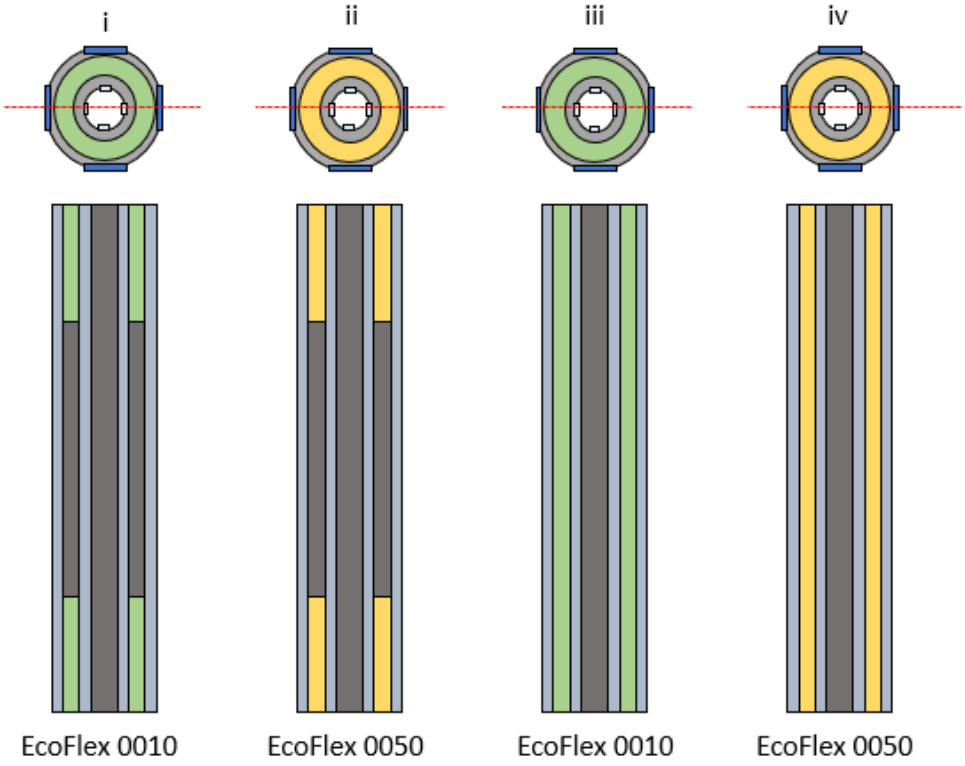

Figure 3.3: *The composition of the 4 physical test pieces.*

Upon physical testing, test piece *i* displaced most appropriately of the four when exposed to the magnitude of force that the end-effector is expected to be subject to (0-100N).

3.2.2. Data Acquisition and processing

Data acquisition is performed using an Arduino. The Arduino reads the voltage output by the 4 Hall Effects sensors. The raw voltage values (which may range between 0 and 1023) are passed through a moving average filter to smooth any measurement noise. A transmission message frame was defined, consisting of 6 bits to begin the message frame followed by 40 bits consisting of the filtered data, shown by figure 3.4:

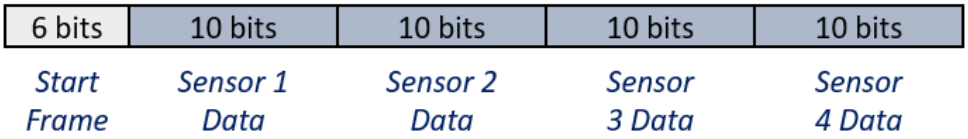

Figure 3.4: *The transmission message frame.*

The message frame is transmitted via serial to the myRIO when a 'send' command is received.

The myRIO sends a transmission request to the Arduino via the serial protocol when a message frame is desired. Upon receipt of the message frame, the first 6 bits and the length of the frame are checked to determine frame validity, where any invalid message frames are discarded. The message frame is then spilt into individual data for each sensor and run through a Neural Network which has been trained to obtain Fx and Fy from the raw voltage values. This architecture is shown by figure 3.5:

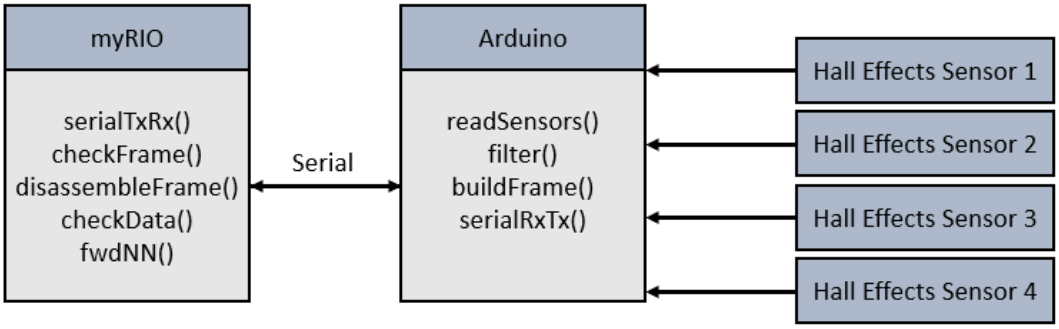

Figure 3.5: *The system architecture for the force sensor.*

A Neural Network was used to convert the raw voltage readings because there was difficulty in modelling the relationship between Hall Effects sensor voltages and input forces. This is because of the non-linear displacements of the hyperelastic silicon material under load and the non-linear relationships between the magnets and the Hall Effects Sensors in a complex 3D configuration.

3.2.3. Training the Neural Network

In order to train the Neural Network, it was necessary to acquire a large amount of data under known loading conditions. To this end, a simple test rig was built. The test piece was clamped to the rig in the same way that it would be attached to the MyPAM, at a known

angle of rotation. A spring balance force gauge was placed between the test piece and the loading point. The test rig is shown by figure 3.6:

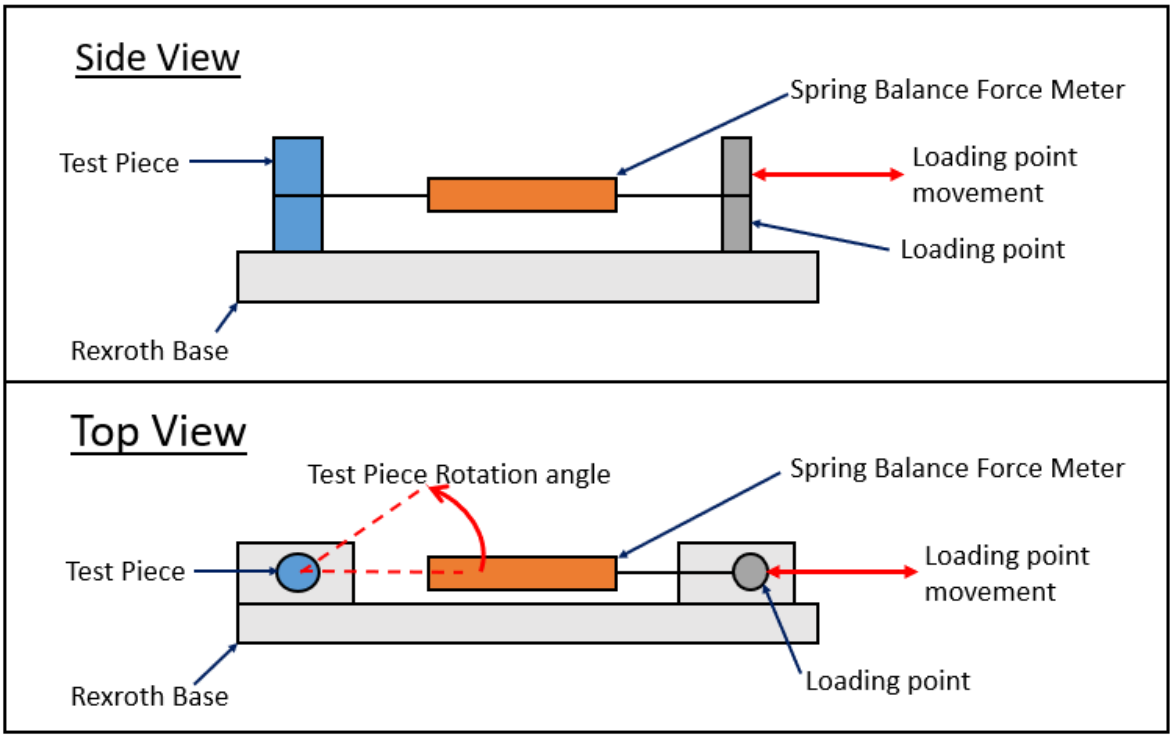

Figure 3.6: *The force sensor test rig.*

The Hall Effects sensor raw voltage outputs were logged along with the force displayed on the spring balance force gauge and the rotation angle of the test piece. The loading point was moved to increase the force in increments of 5N, and readings were logged at each force increment. The rotation angle was increased, and the loading process repeated. This process was repeated with the test piece rotated to different angles until a full revolution had been completed. The result of this was a training data set of just under 8000 data points, which took the form shown by table 3.4:

Input Force (N)	Test Piece Rotation (deg)	Sensor 1 Raw Bits	Sensor 2 Raw Bits	Sensor 3 Raw Bits	Sensor 4 Raw Bits
0	0	540	541	542	539

Table 3.4: *The format of the training data.*

A number of Neural Networks with various topologies were trained in MATLAB. By necessity the networks had 4 input neurons, 1 for the raw voltage data from each Hall Effects sensor, and 2 output neurons, for Fx and Fy. The Neural Network that most successfully struck the balance between acceptable error and computational speed had 2 hidden layers. The first hidden layer had 20 neurons and the second hidden layer had 10 neurons. Each neuron performed a sigmoid-tangent calculation for the threshold function because the output of the neural network was expected to produce both negative and positive Force outputs. The weights and biases were then extracted so that the network

could be rebuilt on the myRIO in LabVIEW, and thus convert the raw voltage outputs into Fx and Fy in real time. The topology of the Neural Network is shown by figure 3.7:

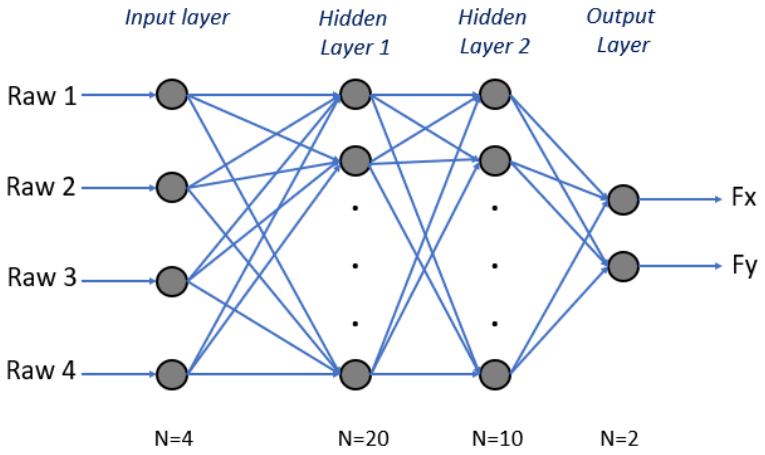

Figure 3.7: *topology of the trained Neural Network.*

3.2.4. Force Sensor Validation and Limitations

The force sensor has not been validated beyond further testing using the test rig and analysis of training data error, however the outcome of this testing is promising and warrants further work. There remains some measurement error following the training of the Neural Network. Figure 3.8 shows X and Y force components predicted by the Neural Network plotted against the actual X and Y force components for the training data:

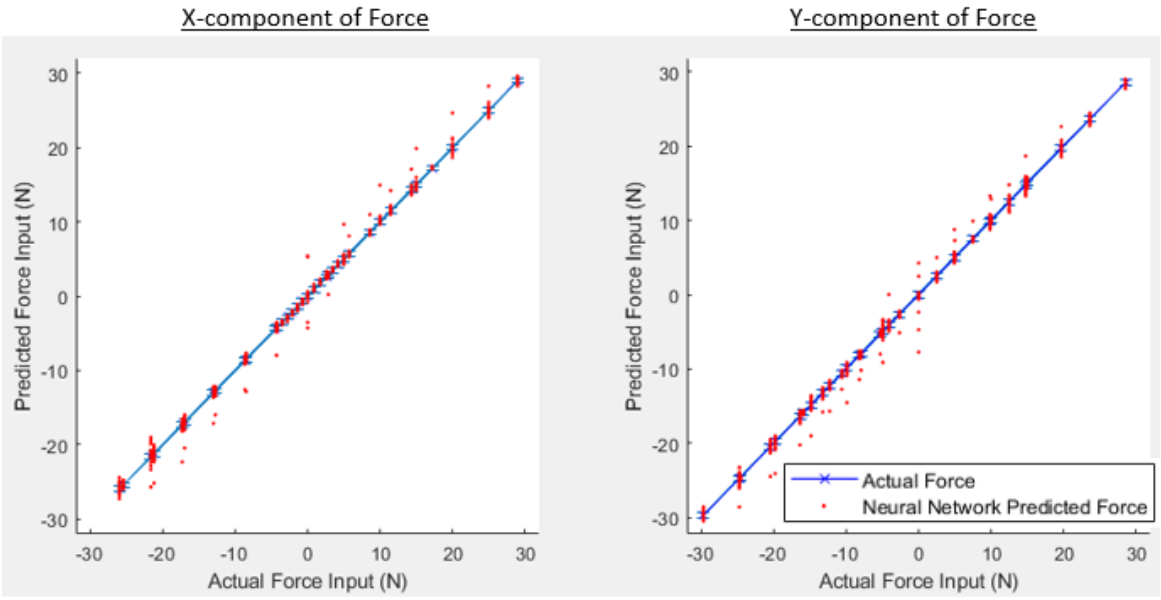

Figure 3.8: *Force prediction of the Neural Network vs Actual Force.*

It can be seen that there are points where the error is large, with the largest error of -7.73N. The mean magnitude of error across the training data was 0.185N in the X direction and 0.218N in the Y direction. When investigating the training data where the errors were large it was noted that the raw voltage values were not of the expected magnitude. Due to

the physical configuration of the force sensor, the raw voltage values from each Hall Effects sensor should be above 512, where 512 indicates that no magnetic field is detected and 1023 indicates a saturation of the Hall Effects sensor with a North aligned magnetic field. The training data where the errors were large had raw voltage outputs of less than 512 as shown by table 3.5:

Input Force (N)	Test Piece Rotation (deg)	Sensor 1 Raw Bits	Sensor 2 Raw Bits	Sensor 3 Raw Bits	Sensor 4 Raw Bits
0	90	432	539	540	542

Table 3.5: *Training data with errors.*

This indicates the detection of a South aligned magnetic field, an impossibility with the configuration of the force sensor where all of the magnets have the North face aligned with the Hall Effects Sensors as shown by figure 3.2. The force measurement errors are likely to have arisen from a number of areas:

1. The Arduino is being utilised at maximum processing capacity, which means that it may be the case that at some points measurements are not fully completed and processed before transmission.
2. The test piece consists of unshielded wires with a potentially poor connection, making the measurements susceptible to excessive noise.
3. The test piece was hand built to a poor level of accuracy, with the Hall Effects sensors not correctly aligned with the corresponding magnets.
4. The data collection was performed manually with a spring balance force meter of poor resolution and a protractor to measure the rotation of the test piece. Measurement accuracy and resolution were poor compared with what can be expected from a full automated test rig.

With these build and testing limitations identified, the force predicted by the Neural Network is of a reasonable level of accuracy and the concept has been proven enough to justify further work in this area, which is discussed in section 4.2 of this report.

3.3. Implementing Admittance Control

Admittance control was selected over Impedance control as the first form of interaction control to implement because it is based on an inner position loop. This has two key benefits: the kinetics of the MyPAM can be ignored and it means that force is only required to be measured at the end effector, rather than at each joint. An Admittance control scheme for MyPAM was designed according to figure 2.6 in section 2.4.5. This is shown by the block diagram in figure 3.9:

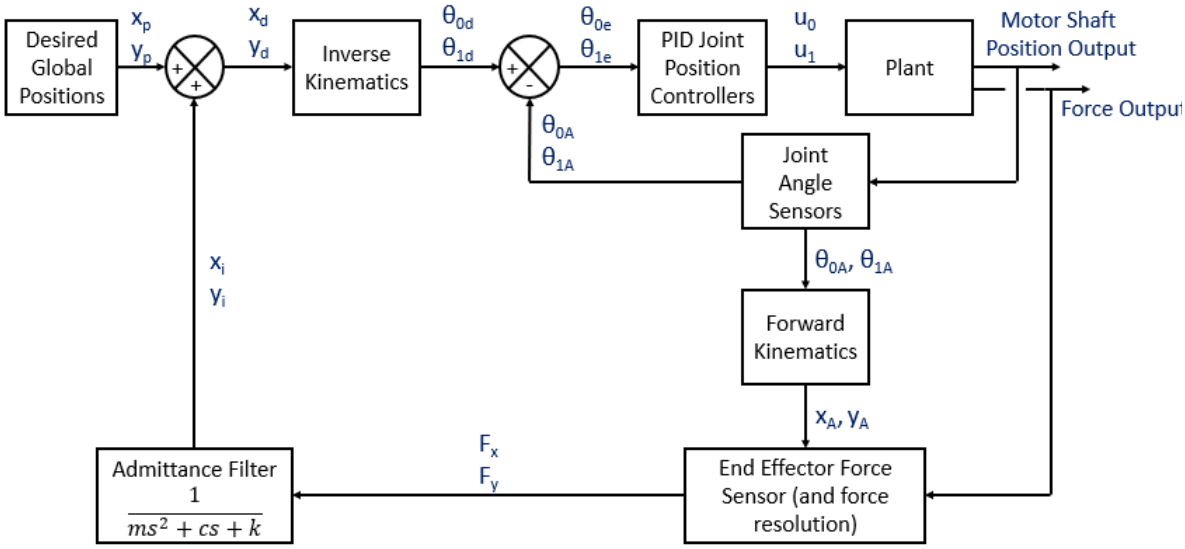

Figure 3.9: *A block diagram for the Admittance control scheme.*

It may be seen in figure 3.9 that the interaction force between the end effector and the patient is resolved into its X and Y force components, which ensures that the force is known with reference to the global frame before being passed through the Admittance filter. The position demands, x_i and y_i, are used to modulate the global position demands x_p and y_p. This produces x_d and y_d, which are then transformed into the motor angle demands by inverse kinematics. The motor angle demands are then used for position PID control in the traditional way. The inverse kinematics for the MyPAM may be found in Appendix B.

3.3.1. The Admittance Filter

The Admittance filter is a virtual mass-spring-damper arrangement and takes the form shown by equation 3.25, where *m* represents the virtual mass, *c* represents the virtual damping and *k* represents the virtual stiffness:

$$x_i = \frac{F_x}{ms^2 + cs + k} \tag{3.25}$$

Mass was omitted since it does not provide any benefits in this model, thus a simplified spring-damper arrangement was used. The force input to the Admittance filter may be considered as a step input. This means that the Admittance filter is applied in the control code on the myRIO as shown by equation 3.26, the derivation of which may be found in Appendix C:

$$\mathrm{x}_i(\mathrm{t}) = \frac{1}{k} F_x \left(1 - e^{-\frac{k}{c}t}\right) \tag{3.26}$$

Where $x_i(t)$ is the position adjustment in the x direction required at time t, k is the sitffness coefficient, c is the damping coefficient, t is the time and F_x is the x component of force.

Using equation 3.26, a difficulty is presented by the selection of a value of time to used for *t*. This is unclear because the Admittance filter requires instantaneous values for

force that change unpredictably, and the value for force will not be constant across the time needed until decomposition. A number of options exist:

- Option 1: Assume that time *t* is very large. This means that as time *t* tends to infinity, the exponential term in equation 3.26 tends to 0, which has the effect of entirely removing the damping coefficient *c* from the equation and the Admittance filter acts simply as a virtual spring. The same result is found by applying the final value theorem to the standard form of equation 3.26.
- Option 2: Monitor the force input value, and if it is the same for a number of iterations (within limits) increase the value for time *t* from t=0. If the force changes, reset the value to *t*=0.This has the potential to render the Admittance filter useless. For example, if the force input changes quickly, then the filter will always be acting at time t=0, thus not modulating the position at all since $x_i(t) = 0$ when t=0.
- Option 3: Apply the filter with a small damping coefficient *c* ensuring a quick decay. This has the same effect as option 1, where the exponential term in equation 3.26 tends to 0 and the Admittance filter acts simply as a virtual spring.
- Option 4: Use a static value for time *t*. This is the preferred option, since it reduces the programming complexity, but it also allows for the stiffness coefficient *k* to be changed dynamically to different levels of assistance to be provided to the patient.

Option 4 was selected, though the coefficients *t*, *c*, and *k* must be heuristically determined. This also allows the level of assistance provided to the patient may be dynamically altered by changing the value for coefficient *k,* which was the strategy adopted by Culmer et al (2010). With a constant value for *t* and *c*, the level of assistance may be raised by lowering the value for *k*, as shown by figure 3.10 where a step input of 10N was input into 2 virtual spring damper arrangements:

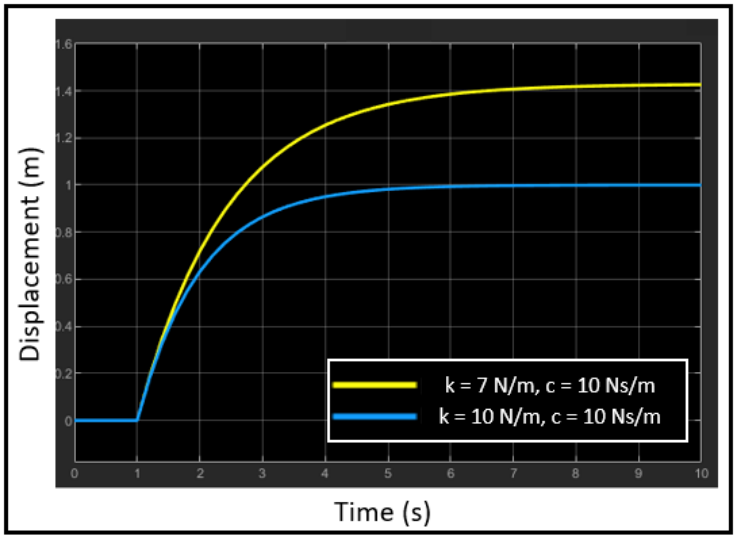

Figure 3.10: *Increasing assistance by lowering the stiffness coefficient k.*

It can be seen in figure 3.10 that any value of time *t*, the displacement is greater for the spring-damper with stiffness coefficient *k* = 7N/m than the spring-damper with stiffness coefficient *k* = 10N/m, thus providing a greater level of assistance.

The framework of the Admittance control strategy has been programmed on the myRIO as the low-level control strategy, but work remains to test and validate this. Two Admittance filters were implemented, the first converts the X component of force into a desired X displacement and the second converts the Y component of force into a desired Y displacement. Usefully this corresponds well with the Minimum Jerk Trajectory generator which is similarly implemented twice, once for the X direction and once for the Y direction. This is further discussed in section 4.3 of this report.

Chapter 4: Future Work

4.1. Trajectory Integration and Validation

As part of the design of the new systems architecture, the specifications for the games have yet to be decided, but currently there is no method for the Minimum Jerk Trajectory to be generated by the game. Indeed, there are situations when the game must produce the trajectory, such as circle tracking, and situations when the low-level controller must produce the trajectory, such as point-to-point reaching exercises. During the design of the new systems architecture a system must be set up to communicate whether the game (the high-level controller) or the myRIO (the low-level controller) is responsible of generating the trajectory. Further to this, a software watchdog must be created to ensure that no dangerous situations occur whilst responsibility is being exchanged between the 2 controllers.

With the architecture designed and implemented, the Minimum Jerk Trajectory generated by the low-level controller must be validated. The first part of this is ensuring that communication is working correctly so that only with the correct game types is the Minimum Jerk Trajectory generated and implemented by the low-level controller, and also that if communication is lost then the entire system enters a safe state.

The final part of the trajectory generation is the integration of a system whereby Attractors and Repulsors may be defined by the game. An Attractor is defined here as a point in cartesian space which attracts the end-effector/handle towards it, much like a gravity well. A Repulsor is defined here as a point in cartesian space which repulses the end-effector/handle away from it. Both the Attractors and Repulsors must generate virtual forces between themselves and the end-effector proportional to the distance between themselves and the end-effector, which will clearly have an effect on the trajectory generated. It is anticipated that these may be implemented either as an additional Impedance or Admittance filter.

4.2. Force Sensor

In section 3.2 it was shown that a low-cost force sensor was capable of measuring the X and Y components of force, but there was an unacceptable level of inaccuracy in these measurements. Further work is required to finalise and validate the force sensor and to limit the measurement inaccuracy.

It was discussed that the Arduino was operating at its maximum processing capacity, occasionally and unpredictably transmitting incomplete data. This will be resolved by replacing the Arduino with a much more capable Teensy 3.2 embedded device. The Teensy 3.2 operates 5 times faster than the Arduino and has access to considerably more RAM and Flash memory. Wiring between the Hall Effects sensors, the Teensy 3.2 and the

myRIO will be shielded to prevent measurement noise induced by electromagnetic interference.

The inner and outer rigid cores of the test piece will be professionally manufactured according to technical drawings. The Hall Effects sensors will be accurately positioned with the aid of a 3D printed insert. Importantly, provision has been made for the use of alignment pins, which will ensure that the inner core, outer core and 3D printed insert will be correctly aligned during assembly. The Neodymium magnets will be correctly positioned with the aid of recesses machined into the outer core. Finally, 3D printed inserts at either end of the test piece will ensure the correct distance between the inner and outer cores during the process of casting the EcoFlex™ 0010 hyperelastic silicon material.

An automated test rig will be manufactured, similar in design to the manual test rig. A servomotor will be used to rotate the test piece to a precisely known angle. A second servomotor connected to a lead screw will move the load point relative to the test piece in the horizontal plane. An industrial force meter will be used to detect the force applied to the test piece. Raw voltage readings from the Hall Effects sensors in the test piece will be gathered with force applied to the test piece ranging from 0-50N, increasing by 1N each time. This process will be repeated from 0 degrees of rotation of the test piece to 359 degrees of the test piece, changing by 1 degree each time. This data will form the training data, which will be used to retrain the Neural Network.

With the Neural Network retrained with high quality data, the force sensor will then be validated by applying loads using an Instron Tensile testing machine. The output of the Neural Network will be compared with the input forces to ensure an acceptable level of accuracy is reached by the Neural Network.

4.3. Admittance Control

With the Admittance Control designed, it must be implemented. The first stage is to refine the tuning of the PID position control inner loop, which is currently unstable after the integration of new components. The coefficients for c, k and t in the Admittance filter must be heuristically determined. The Admittance control strategy will then be validated. This involves running the MyPAM through a series of reaching tasks and logging the position, velocity and acceleration data. This data will be compared with data gathered from Optotrak sensors to ensure safe, predictable and reliable operation.

4.4. Impedance Control

The first stage in designing the Impedance control strategy is to refine the dynamic model that has been built, which currently has some inaccuracies due to assumptions that have been made. It was identified in the Literature Review that an accurate dynamic model is necessary to ensure controller stability. With the dynamic model improved, it must be

validated. This will be achieved by comparing the behaviour of the MyPAM with the predicted behaviour of the model. It is anticipated that there will be some difficulty in modelling the friction in the joints, alongside the effects of backlash in the gears.

Low-cost torque sensors will be designed for the joints, applying a methodology similar to the low-cost force sensor designed for the end-effector/handle. Torque sensors are a necessary component required for closed-loop force control.

The Impedance filter must be programmed and implemented on the low-level controller. As part of this process, the Impedance control must be tested and the coefficients for *c*, *k* and *t* in the Impedance filter must be heuristically determined. The Impedance control strategy will then be validated. This involves running the MyPAM through a series of reaching tasks and logging position, velocity, acceleration, Force and Torque data. This data will be compared with model predictions and data gathered from Optotrak sensors to ensure safe, predictable and reliable operation.

4.5. System Re-architecture and Research Interdependencies

With the current highly coupled systems architecture there is no way to separate the trajectory generation from the game. Further to this, the current games are highly dependent on a virtual world which has been built in Unity® software, which limits the development potential for both game development and the interactions between the low-level controller with the high-level controller. To this end, an undergraduate summer internship has been secured to assist with the creation of a software control level addition to the system architecture, which is shown by figure 4.1:

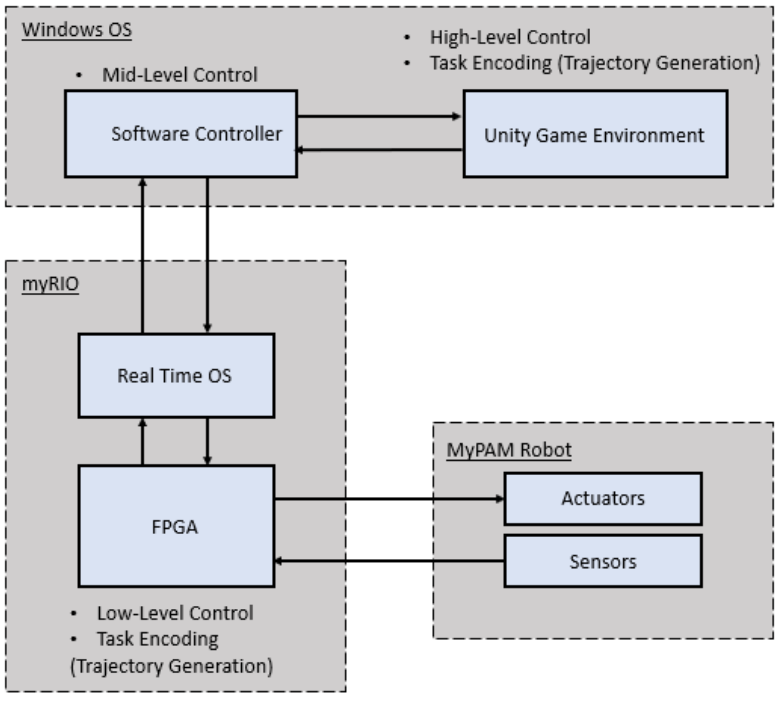

Figure 4.1: *The revised system architecture.*

The addition of a mid-level control system, responsible for establishing communication, monitoring safety, data logging, and determining trajectory generation responsibilities opens up possibilities for redesigning the game architecture. To this end, a further undergraduate summer internship has been established to define the specifications for game design. This will ensure maintainability, scalability and testability of game development in the future. The author of this report has some supervisory responsibility over the undergraduate summer internships.

In the longer term it is planned that all National Instruments products will be replaced. This is anticipated to remove significant cost from the manufacture of the MyPAM.

4.6. Human-based testing

The final stage is the human-based testing. The tests have yet to be defined, and this stage is dependent on the final outcome of funding which was successfully campaigned for. Ideally a full clinical trial will be undertaken, with a multidisciplinary team of clinicians and physiotherapists involved in the design of the study. It is anticipated that such a clinical trial would focus on the comparison of the rehabilitation outcomes of patients, some of whom will be using MyPAM devices with an Admittance controller, some of whom will be using MyPAM devices with an Impedance controller, and a control group who will undergo traditional physiotherapy with no access to rehabilitation robotics. Once the study is complete, data analysis must be performed to determine whether rehabilitation outcomes can be correlated with access to rehabilitation robotics.

4.7. Work Plan

Figure 4.2 shows a Gantt chart of the projected work plan:

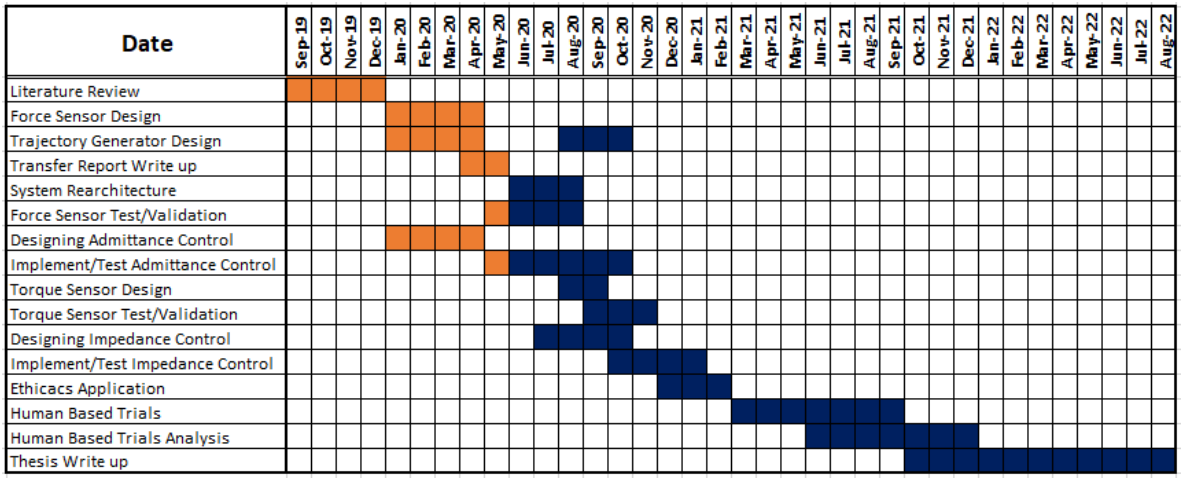

Figure 4.2: *A Gantt chart of the projected work plan.*

4.8. Conclusion

It is clear that there is a requirement for low-cost rehabilitation robotics, since the main issue with the current cohort of commercially available rehabilitation robotic is the high cost of devices and the low cost to benefit ratio. The MyPAM is a low-cost rehabilitation robot designed for the rehabilitation of Stroke patients in a home environment. Currently the MyPAM uses position control as the low-level control scheme, and there is a high level of coupling between the high-level control strategy and low-level control implementation. The design and implementation of some form of interaction control for the MyPAM has the potential to extend the use of the MyPAM to patients with lower levels of motor control. The interaction control schemes to be investigated are Admittance control and Impedance control.

The Admittance control scheme for MyPAM has been designed and programmed on the myRIO using LabVIEW, but the position PID inner loop requires further tuning and the *c*, *k* and *t* coefficients in the Admittance filter have yet to be heuristically determined. Full testing of the Admittance control scheme relies upon the use of a force sensor to determine robot-patient interaction forces.

It has been shown that the use of a smooth trajectory is useful in preventing dangerous interaction forces between the robot and the patient. A Minimum Jerk Trajectory generator has been programmed on the myRIO using LabVIEW. The full implementation will be achieved once the software control layer has been built during the system rearchitecture, which will determine when the low-level controller is in control of the trajectory and when the high-level controller (game) is in control of the trajectory.

A prototype force low-cost force sensor has been built, and the results of testing are promising, which justify the production of a high-quality final product and an automated test rig. The final product requires validation, which is planned on an Instron Tensile testing machine. The lessons learned from the development of the low-cost force sensor are likely to transfer to the development of the low-cost torque sensor, which will allow the development of the Impedance control scheme.

It remains to finalise the development and testing the low-level control schemes such that MyPAM can be prepared for human based tests, based on the outcome of an ethical application and funding.

Chapter 5: References

- Amirabdollahian, F., Loureiro, R. and Harwin, W., 2002. Minimum jerk trajectory control for rehabilitation and haptic applications. In *Proceedings 2002 IEEE International Conference on Robotics and Automation (Cat. No. 02CH37292)* (Vol. 4, pp. 3380-3385). IEEE.
- Anderson, R.J. and Spong, M.W., 1988. Hybrid impedance control of robotic manipulators. *IEEE Journal on Robotics and Automation*, *4*(5), pp.549-556.
- Balasubramanian, S., Melendez-Calderon, A., Roby-Brami, A. and Burdet, E., 2015. On the analysis of movement smoothness. *Journal of NeuroEngineering and rehabilitation*, *12*(1), p.112.
- Burgar, C.G., Lum, P.S., Shor, P.C. and Van der Loos, H.M., 2000. Development of robots for rehabilitation therapy: The Palo Alto VA/Stanford experience. *Journal of rehabilitation research and development*, *37*(6), pp.663-674.
- Coleman, E.R., Moudgal, R., Lang, K., Hyacinth, H.I., Awosika, O.O., Kissela, B.M. and Feng, W., 2017. Early rehabilitation after stroke: a narrative review. *Current atherosclerosis reports*, *19*(12), p.59.
- Culmer, P., Jackson, A., Richardson, R., Bhakta, B., Levesley, M. and Cozens, A., 2005, June. Development of a dual robotic system for upper-limb stroke rehabilitation. In *9th International Conference on Rehabilitation Robotics, 2005. ICORR 2005.*(pp. 61-65). IEEE.
- Culmer, P.R., 2007. *Development of a Cooperative Robot System to Aid Stroke Rehabilitation* (Doctoral dissertation, University of Leeds).
- Culmer, P.R., Jackson, A.E., Makower, S., Richardson, R., Cozens, J.A., Levesley, M.C. and Bhakta, B.B., 2010. A control strategy for upper limb robotic rehabilitation with a dual robot system. *IEEE/ASME Transactions on Mechatronics*, *15*(4), pp.575-585.
- Duffau, H., 2006. Brain plasticity: from pathophysiological mechanisms to therapeutic applications. *Journal of clinical neuroscience*, *13*(9), pp.885-897.
- Erol, D. and Sarkar, N., 2007. Design and Implementation of a Control Architecture for Rehabilitation Robotic Systems. In *Rehabilitation Robotics*. InTech.
- Firouzy, S., 2011. *Control Algorithms to Improve the Dynamic Performance of Robotic Rehabilitation Devices* (Masters dissertation, University of Leeds (School of Mechanical Engineering)).
- Flash, T. and Hogan, N., 1985. The coordination of arm movements: an experimentally confirmed mathematical model. *Journal of neuroscience*, *5*(7), pp.1688-1703.
- Hogan, N. and Buerger, S.P., 2004. Impedance and interaction control. In *Robotics and automation handbook* (pp. 375-398). CRC Press.
- Hogan, N., 1984, June. Impedance control: An approach to manipulation. In *American Control Conference, 1984* (pp. 304-313). IEEE.
- Hogan, N., 1984. Impedance control of industrial robots. *Robotics and Computer-Integrated Manufacturing*, *1*(1), pp.97-113.
- Hogan, N., Krebs, H.I., Charnnarong, J., Srikrishna, P. and Sharon, A., 1992, September. MIT-MANUS: a workstation for manual therapy and training. I. In *[1992] Proceedings IEEE International Workshop on Robot and Human Communication*(pp. 161-165). IEEE.
- Hogan, N., Krebs, H.I., Sharon, A. and Charnnarong, J., Massachusetts Institute of Technology, 1995. *Interactive robotic therapist*. U.S. Patent 5,466,213.
- Jackson, A., Culmer, P., Makower, S., Levesley, M., Richardson, R., Cozens, A., Williams, M.M. and Bhakta, B., 2007, June. Initial patient testing of iPAM-a robotic system for stroke rehabilitation. In *2007 IEEE 10th International Conference on Rehabilitation Robotics* (pp. 250-256). IEEE.
- Jackson, A.E., Holt, R.J., Culmer, P.R., Makower, S.G., Levesley, M.C., Richardson, R.C., Cozens, J.A., Williams, M.M. and Bhakta, B.B., 2007. Dual robot system for upper limb rehabilitation after stroke: the design process. *Proceedings of the Institution of Mechanical Engineers, Part C: Journal of Mechanical Engineering Science*, *221*(7), pp.845-857.
- Johnson, M.J., Feng, X., Johnson, L.M. and Winters, J.M., 2007. Potential of a suite of robot/computer-assisted motivating systems for personalized, home-based, stroke rehabilitation. *Journal of NeuroEngineering and Rehabilitation*, *4*(1), p.6.

- Kahn, L.E., Zygman, M.L., Rymer, W.Z. and Reinkensmeyer, D.J., 2006. Robot-assisted reaching exercise promotes arm movement recovery in chronic hemiparetic stroke: a randomized controlled pilot study. *Journal of NeuroEngineering and rehabilitation*, *3*(1), p.12.
- Krebs, H.I., Ferraro, M., Buerger, S.P., Newbery, M.J., Makiyama, A., Sandmann, M., Lynch, D., Volpe, B.T. and Hogan, N., 2004. Rehabilitation robotics: pilot trial of a spatial extension for MIT-Manus. *Journal of NeuroEngineering and Rehabilitation*, *1*(1), p.5.
- Krebs, H.I., Hogan, N., Aisen, M.L. and Volpe, B.T., 1998. Robot-aided neurorehabilitation. *IEEE transactions on rehabilitation engineering*, *6*(1), pp.75-87.
- Kreisel, S.H., Hennerici, M.G. and Bäzner, H., 2007. Pathophysiology of stroke rehabilitation: the natural course of clinical recovery, use-dependent plasticity and rehabilitative outcome. *Cerebrovascular diseases*, *23*(4), pp.243-255.
- Lawrence, E.S., Coshall, C., Dundas, R., Stewart, J., Rudd, A.G., Howard, R. and Wolfe, C.D., 2001. Estimates of the prevalence of acute stroke impairments and disability in a multiethnic population. *Stroke*, *32*(6), pp.1279-1284.
- Lee, R.D. and Mason, A. eds., 2011. *Population aging and the generational economy: A global perspective*. Edward Elgar Publishing.
- Lee, S., Bae, S., Jeon, D. and Kim, K.Y., 2015. The effects of cognitive exercise therapy on chronic stroke patients' upper limb functions, activities of daily living and quality of life. *Journal of physical therapy science*, *27*(9), pp.2787-2791.
- Liu, Y., Li, C., Ji, L., Bi, S., Zhang, X., Huo, J. and Ji, R., 2017. Development and implementation of an end-effector upper limb rehabilitation robot for hemiplegic patients with line and circle tracking training. *Journal of healthcare engineering*, *2017*.
- Lum, P.S., Burgar, C.G., Van der Loos, M. and Shor, P.C., 2006. MIME robotic device for upper-limb neurorehabilitation in subacute stroke subjects: A follow-up study. *Journal of rehabilitation research and development*, *43*(5), p.631.
- Lum, P.S., Burgar, C.G., Van der Loos, M., Shor, P.C., Majmundar, M. and Yap, R., 2005, June. The MIME robotic system for upper-limb neurorehabilitation: results from a clinical trial in subacute stroke. In *9th International Conference on Rehabilitation Robotics, 2005. ICORR 2005.* (pp. 511-514). IEEE.
- Maciejasz, P., Eschweiler, J., Gerlach-Hahn, K., Jansen-Troy, A. and Leonhardt, S., 2014. A survey on robotic devices for upper limb rehabilitation. *Journal of NeuroEngineering and rehabilitation*, *11*(1), p.3.
- Marchal-Crespo, L. and Reinkensmeyer, D.J., 2009. Review of control strategies for robotic movement training after neurologic injury. *Journal of NeuroEngineering and rehabilitation*, *6*(1), p.20.
- Marek, S.M., Cramer, J.T., Fincher, A.L., Massey, L.L., Dangelmaier, S.M., Purkayastha, S., Fitz, K.A. and Culbertson, J.Y., 2005. Acute effects of static and proprioceptive neuromuscular facilitation stretching on muscle strength and power output. *Journal of athletic training*, *40*(2), p.94.
- Micera, S., Carrozza, M.C., Guglielmelli, E., Cappiello, G., Zaccone, F., Freschi, C., Colombo, R., Mazzone, A., Delconte, C., Pisano, F. and Minuco, G., 2005. A simple robotic system for neurorehabilitation. *Autonomous Robots*, *19*(3), p.271.
- Montagner, A., Frisoli, A., Borelli, L., Procopio, C., Bergamasco, M., Carboncini, M.C. and Rossi, B., 2007, September. A pilot clinical study on robotic assisted rehabilitation in VR with an arm exoskeleton device. In *2007 Virtual Rehabilitation* (pp. 57-64). IEEE.
- Morreale, M., Marchione, P., Pili, A., Lauta, A., Castiglia, S.F., Spallone, A., Pierelli, F. and Giacomini, P., 2016. Early versus delayed rehabilitation treatment in hemiplegic patients with ischemic stroke: proprioceptive or cognitive approach. *European Journal of Physical and Rehabilitation Medicine*, *52*(1), pp.81-9.
- Moskowitz, M.A., Lo, E.H. and Iadecola, C., 2010. The science of stroke: mechanisms in search of treatments. *Neuron*, *67*(2), pp.181-198.
- Office for National Statistics. 2018. *Overview of the UK population: November 2018*. [Online]. [Accessed 13 November 2018]. Available from: https://www.ons.gov.uk/peoplepopulationandcommunity/populationandmigration/populationestimates/articles/overviewoftheukpopulation/november2018
- O'Mahony, P.G., Thomson, R.G., Dobson, R., Rodgers, H. and James, O.F., 1999. The prevalence of stroke and associated disability. *Journal of public health*, *21*(2), pp.166-171.

- Ott, C., Mukherjee, R. and Nakamura, Y., 2010, May. Unified impedance and admittance control. In *2010 IEEE International Conference on Robotics and Automation* (pp. 554-561). IEEE.
- Patton, J.L., Stoykov, M.E., Kovic, M. and Mussa-Ivaldi, F.A., 2006. Evaluation of robotic training forces that either enhance or reduce error in chronic hemiparetic stroke survivors. *Experimental brain research*, *168*(3), pp.368-383.
- Reinkensmeyer, D.J., Takahashi, C.D., Timoszyk, W.K., Reinkensmeyer, A.N. and Kahn, L.E., 2001. Design of robot assistance for arm movement therapy following stroke. *Advanced robotics*, *14*(7), pp.625-637.
- Richardson, M.J. and Flash, T., 2002. Comparing smooth arm movements with the two-thirds power law and the related segmented-control hypothesis. *Journal of neuroscience*, *22*(18), pp.8201-8211.
- Richardson, R., 2001. *Actuation and control for robotic physiotherapy* (Doctoral dissertation, University of Leeds).
- Richardson, R., Brown, M., Bhakta, B. and Levesley, M.C., 2003. Design and control of a three degree of freedom pneumatic physiotherapy robot. *Robotica*, *21*(6), pp.589-604.
- Richardson, R., Jackson, A., Culmer, P., Bhakta, B. and Levesley, M.C., 2006. Pneumatic impedance control of a 3-dof physiotherapy robot. *Advanced Robotics*, *20*(12), pp.1321-1339.
- Rodgers, H., Bosomworth, H., Krebs, H.I., van Wijck, F., Howel, D., Wilson, N., Aird, L., Alvarado, N., Andole, S., Cohen, D.L. and Dawson, J., 2019. Robot assisted training for the upper limb after stroke (RATULS): a multicentre randomised controlled trial. *The Lancet*.
- Sanchez, R.J., Wolbrecht, E., Smith, R., Liu, J., Rao, S., Cramer, S., Rahman, T., Bobrow, J.E. and Reinkensmeyer, D.J., 2005, June. A pneumatic robot for re-training arm movement after stroke: Rationale and mechanical design. In *9th International Conference on Rehabilitation Robotics, 2005. ICORR 2005.* (pp. 500-504). IEEE.
- Sivan, M., Gallagher, J., Makower, S., Keeling, D., Bhakta, B., O'Connor, R.J. and Levesley, M., 2014. Home-based Computer Assisted Arm Rehabilitation (hCAAR) robotic device for upper limb exercise after stroke: results of a feasibility study in home setting. *Journal of NeuroEngineering and rehabilitation*, *11*(1), p.163.
- Sommerfeld, D.K., Eek, E.U.B., Svensson, A.K., Holmqvist, L.W. and von Arbin, M.H. 2004. Spasticity after stroke: its occurrence and association with motor impairments and activity limitations. *Stroke*, 35(1), pp.134-139
- Stroke Association. 2017. *Current, future and avoidable costs of stroke in the UK*. [Online]. London: Stroke Association. [Accessed 20 November 2018]. Available from: https://www.stroke.org.uk/sites/default/files/costs_of_stroke_in_the_uk_report_-executive_summary_part_2.pdf
- Stroke Association. 2018. *State of the Nation. Stroke Statistics February 2018*. [Online]. London: Stroke Association. [Accessed 13 November 2018]. Available from: https://www.stroke.org.uk/system/files/sotn_2018.pdf
- Stroke Association. 2018. *Using Robotics to help arm, wrist & hand recovery after Stroke*. [Online]. London: Stroke Association. [Accessed 26 November 2018]. Available from: https://www.stroke.org.uk/news/using-robotics-help-arm-wrist-hand-recovery-after-stroke
- Sugar, T.G., He, J., Koeneman, E.J., Koeneman, J.B., Herman, R., Huang, H., Schultz, R.S., Herring, D.E., Wanberg, J., Balasubramanian, S. and Swenson, P., 2007. Design and control of RUPERT: a device for robotic upper extremity repetitive therapy. *IEEE transactions on neural systems and rehabilitation engineering*, *15*(3), pp.336-346.
- Sulzer, J.S., Peshkin, M.A. and Patton, J.L., 2007, June. Design of a mobile, inexpensive device for upper extremity rehabilitation at home. In *2007 IEEE 10th International Conference on Rehabilitation Robotics* (pp. 933-937). IEEE.
- Van Peppen, R.P., Kwakkel, G., Wood-Dauphinee, S., Hendriks, H.J., Van der Wees, P.J. and Dekker, J., 2004. The impact of physical therapy on functional outcomes after stroke: what's the evidence?. *Clinical rehabilitation*, *18*(8), pp.833-862.
- Volpe, B.T., Krebs, H.I., Hogan, N., Edelsteinn, L., Diels, C.M. and Aisen, M.L., 1999. Robot training enhanced motor outcome in patients with stroke maintained over 3 years. *Neurology*, *53*(8), pp.1874-1874.
- Wang, H., De Boer, G., Kow, J., Alazmani, A., Ghajari, M., Hewson, R. and Culmer, P., 2016. Design methodology for magnetic field-based soft tri-axis tactile sensors. *Sensors*, *16*(9), p.1356.

- Xu, X.M., Vestesson, E., Paley, L., Desikan, A., Wonderling, D., Hoffman, A., Wolfe, C.D., Rudd, A.G. and Bray, B.D., 2018. The economic burden of stroke care in England, Wales and Northern Ireland: Using a national stroke register to estimate and report patient-level health economic outcomes in stroke. *European Stroke Journal*, *3*(1), pp.82-91.

Appendices

Appendix A: Calculating the Minimum Jerk Trajectory using Calculus of Variations

For a Minimum Jerk Trajectory, $L = (\dddot{x})^2$ (Flash and Hogan,1985). Using Equation 3.1:

$$x^*(t) = F(x(t)) = argmin_{x(t)} \int_0^T (\dddot{x})^2 \, dt \tag{A.1}$$

$$F(x(t)) = \frac{1}{2}\int_0^T (\dddot{x})^2 \, dt \tag{A.2}$$

Multiplying through by ½ simplifies the maths later on.

Introducing a small variation, $\gamma(t)$, which has the following properties:

$$\begin{aligned} \gamma(0) &= 0, \quad & \gamma(T) &= 0 \\ \dot{\gamma}(0) &= 0, \quad & \dot{\gamma}(T) &= 0 \\ \ddot{\gamma}(0) &= 0, \quad & \ddot{\gamma}(T) &= 0 \end{aligned} \tag{A.3}$$

To minimise $F(x(t))$, add $\gamma(t)$ as a variation:

$$x(t) = x(t) + e\gamma(t) \tag{A.4}$$

$$F(x + e\gamma) = \frac{1}{2}\int_0^T (\dddot{x} + e\dddot{\gamma})^2 \, dt \tag{A.5}$$

Differentiating with respect to γ:

$$\frac{dF(x + e\gamma)}{e} = \int_0^T (\dddot{x} + e\dddot{\gamma})\ddot{\gamma} \, dt \tag{A.6}$$

$$\left.\frac{dF(x + e\gamma)}{e}\right|_{e=0} = \int_0^T \dddot{x}\ddot{\gamma} \, dt \tag{A.7}$$

Integrating by parts:

$$\int_0^T \dddot{x}\ddot{\gamma} \, dt = \int_0^T u \, dv = [uv]_0^T - \int_0^T v \, du \tag{A.8}$$

Where:

$$\begin{aligned} u &= \ddot{x}, \quad & dv &= \ddot{\gamma} \, dt \\ du &= x^{(4)} dt, \quad & v &= \dot{\gamma} \end{aligned} \tag{A.9}$$

Thus:

$$\int_0^T \dddot{x}\ddot{\gamma} \, dt = \gamma \, [\ddot{x}\,\dot{\gamma}]_0^T - \int_0^T \dot{\gamma} \, x^{(4)} dt = -\int_0^T \dot{\gamma} \, x^{(4)} dt \tag{A.10}$$

Integrating by parts again:

$$-\int_0^T \dot{\gamma} \, x^{(4)} dt = -\int_0^T u \, dv = -[uv]_0^T + \int_0^T v \, du \tag{A.11}$$

Where:

$$u = x^{(4)}, \qquad dv = \ddot{\gamma}\, dt$$
$$du = x^{(5)} dt, \qquad v = \dot{\gamma} \tag{A.12}$$

Thus:

$$-\int_0^T \ddot{\gamma}\, x^{(4)} dt = -\left[x^{(4)}\dot{\gamma}\right]_0^T + \int_0^T \dot{\gamma}\, x^{(5)} dt = \int_0^T \dot{\gamma}\, x^{(5)} dt \tag{A.13}$$

Integrating by parts a final time:

$$\int_0^T \dot{\gamma}\, x^{(5)} dt = \int_0^T u\, dv = [uv]_0^T - \int_0^T v\ du \tag{A.14}$$

Where:

$$u = x^{(5)}, \qquad dv = \dot{\gamma}\, dt$$
$$du = x^{(6)} dt, \qquad v = \gamma \tag{A.15}$$

Thus:

$$\int_0^T \dot{\gamma}\, x^{(5)} dt = \left[x^{(5)}\gamma\right]_0^T - \int_0^T \gamma\, x^{(6)} dt = -\int_0^T \gamma\, x^{(6)} dt \tag{A.16}$$

Finally producing:

$$\left.\frac{dF(x+e\gamma)}{e}\right|_{e=0} = -\int_0^T \gamma\, x^{(6)} dt \equiv 0 \tag{A.17}$$

Since this must hold true for any function of $\gamma(t)$ which has the properties specified above, this means that Equation A.18 must be true:

$$x^{(6)}(t) = 0 \tag{A.18}$$

Which may then be solved for as shown in section 3.12 of this report to provide the Minimum Jerk Trajectory.

Appendix B: Calculating the Inverse Kinematics for the MyPAM

Figure B.1 shows finding the angle at joint 0:

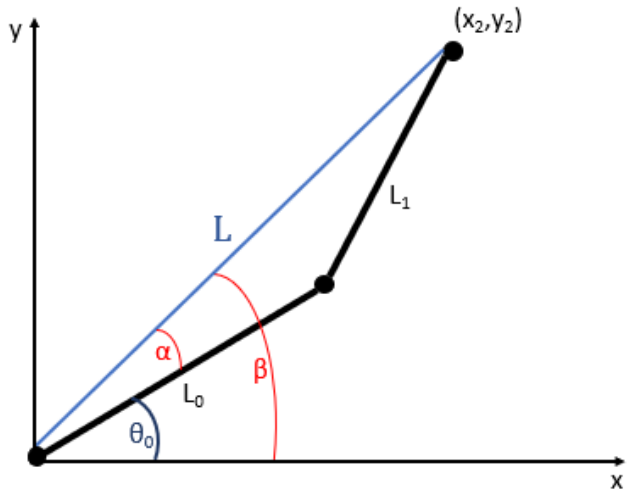

Figure B.1: *Inverse Kinematics for MyPAM, finding the angle at joint 0*

Length L may be found by equation B.1:

$$L = \sqrt{{x_2}^2 + {y_2}^2} \tag{B.1}$$

By the Cosine rule:

$${L_1}^2 = L^2 + {L_0}^2 - 2LL_0 \cos\alpha \tag{B.2}$$

$$\rightarrow \alpha = \cos^{-1}\left(\frac{L^2 + {L_0}^2 - {L_1}^2}{2LL_0}\right) \tag{B.3}$$

$$\beta = \tan^{-1}\left(\frac{y_2}{x_2}\right) \tag{B.4}$$

$$\theta_0 = \beta - \alpha \tag{B.5}$$

Figure B.2 shows finding the angle at joint 1:

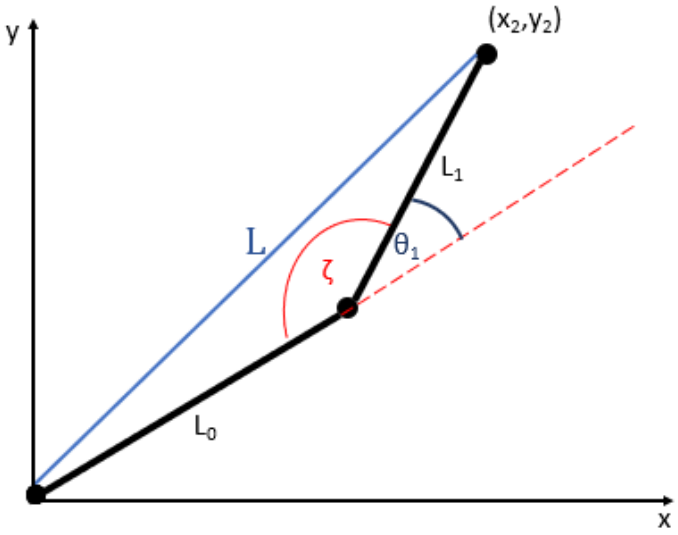

Figure B.2: *Inverse Kinematics for MyPAM, finding the angle at joint 1*

By the Cosine rule:

$$L^2 = {L_0}^2 + {L_1}^2 - 2L_0L_1\cos\zeta \quad (B.6)$$

$$\rightarrow \zeta = \cos^{-1}\left(\frac{{L_0}^2 + {L_1}^2 - L^2}{2L_0L_1}\right) \quad (B.7)$$

$$\theta_1 = 180 - \zeta \quad (B.8)$$

Thus, the desired cartesian position of the end-effector may be transformed into desired joint angles.

Appendix C: Deriving the Admittance Filter Equation

Consider the force input f(t) as a step input with magnitude γ, shown by equation C.1:

$$\mathrm{F(S)} = \mathcal{L}\{\mathrm{f(t)}\} = \frac{\gamma}{s} \tag{C.1}$$

The transfer function G(S) for a spring damper system takes the form shown by equation C.2:

$$G(S) = \frac{A}{1 + \tau s} \tag{C.2}$$

Where $A = \frac{1}{k}$ and $\tau = \frac{c}{k}$.

Thus, the output X(S) is given by equation C.3:

$$X(S) = F(S)G(S) = \frac{A\gamma}{s(1 + \tau s)} \tag{C.3}$$

Partial fraction decomposition:

$$\frac{A\gamma}{s(1 + \tau s)} = \frac{D}{s} + \frac{E}{(1 + \tau s)} \tag{C.4}$$

$$\frac{A\gamma s(1 + \tau s)}{s(1 + \tau s)} = \frac{Ds(1 + \tau s)}{s} + \frac{Es(1 + \tau s)}{(1 + \tau s)} \tag{C.5}$$

$$\frac{A\gamma \cancel{s(1 + \tau s)}}{\cancel{s(1 + \tau s)}} = \frac{D\cancel{s}(1 + \tau s)}{\cancel{s}} + \frac{Es\cancel{(1 + \tau s)}}{\cancel{(1 + \tau s)}} \tag{C.6}$$

$$A\gamma = D(1 + \tau s) + Es \tag{C.7}$$

Collect terms:

$$A\gamma = D + s(D\tau s + E) \tag{C.8}$$

Equating coefficients s^0:

$$D = A\gamma \tag{C.9}$$

Equating coefficients s^1:

$$0 = D\tau + E = A\gamma\tau + E \tag{C.10}$$

$$E = -A\gamma\tau \tag{C.11}$$

Thus:

$$X(S) = \frac{A\gamma}{s(1 + \tau s)} = \frac{A\gamma}{s} - \frac{A\gamma\tau}{1 + \tau s} \tag{C.12}$$

$$\frac{A\gamma}{s} - \frac{A\gamma\tau}{1 + \tau s} = \frac{A\gamma}{s} - \frac{A\gamma\tau}{1 + \tau s} \cdot \frac{1/\tau}{1/\tau} = \frac{A\gamma}{s} - \frac{A\gamma}{s + 1/\tau} \tag{C.13}$$

$$\mathrm{x(t)} = \mathcal{L}^{-1}\{X(S)\} = A\gamma\left(1 - e^{-\frac{1}{\tau}t}\right) \tag{C.14}$$

Finally producing the Admittance relationship shown by equation C.15:

$$\mathrm{x(t)} = \mathcal{L}^{-1}\{X(S)\} = \frac{1}{k}\gamma\left(1 - e^{-\frac{k}{c}t}\right) \tag{C.15}$$